EUKARYOTIC CELL, Oct. 2007, p. 1824–1840 Vol. 6, No. 10
1535-9778/07/$08.00+0 doi:10.1128/EC.00188-07

Role of Actin Cytoskeletal Dynamics in Activation of the Cyclic AMP Pathway and *HWP1* Gene Expression in *Candida albicans*▽†

Michael J. Wolyniak and Paula Sundstrom*

Microbiology and Molecular Pathogenesis Program, Dartmouth Medical School, Hanover, New Hampshire 03755

Received 23 May 2007/Accepted 7 August 2007

Changes in gene expression during reversible bud-hypha transitions of the opportunistic fungal pathogen *Candida albicans* permit adaptation to environmental conditions that are critical for proliferation in host tissues. Our previous work has shown that the hypha-specific adhesin gene *HWP1* is up-regulated by the cyclic AMP (cAMP) signaling pathway. However, little is known about the potential influences of determinants of cell morphology on *HWP1* gene expression. We found that blocking hypha formation with cytochalasin A, which destabilizes actin filaments, and with latrunculin A, which sequesters actin monomers, led to a loss of *HWP1* gene expression. In contrast, high levels of *HWP1* gene expression were observed when the F-actin stabilizer jasplakinolide was used to block hypha formation, suggesting that *HWP1* expression could be regulated by actin structures. Mutants defective in formin-mediated nucleation of F-actin were reduced in *HWP1* gene expression, providing genetic support for the importance of actin structures. Kinetic experiments with wild-type and actin-deficient cells revealed two distinct phases of *HWP1* gene expression, with a slow, actin-independent phase preceding a fast, actin-dependent phase. Low levels of *HWP1* gene expression that appeared to be independent of stabilized actin and cAMP signaling were detected using indirect immunofluorescence. A connection between actin structures and the cAMP signaling pathway was shown using hyper- and hypomorphic cAMP mutants, providing a possible mechanism for up-regulation of *HWP1* gene expression by stabilized actin. The results reveal a new role for F-actin as a regulatory agent of hypha-specific gene expression at the bud-hypha transition.

Candida albicans is an opportunistic fungal pathogen with a tropism for the gastrointestinal mucosa. The progression to candidiasis from the usual state of commensalism is prompted by changes in the immune status of the host that relay signals for proliferation and culminate in tissue invasion. Growth in host tissues is characterized by the presence of yeast, pseudohyphal, and hyphal morphologies in response to a number of environmental parameters within the host that may include temperature, pH, and nutrition (31, 33, 66) as well as other unknown factors. The different morphologies of *C. albicans* are accompanied by differences in gene expression patterns that are critical to the development of candidiasis. The mechanisms that mediate changes in gene expression in concert with changes in morphology are directly relevant to the regulation of virulence of *C. albicans.*

The hypha-specific gene *HWP1* (*h*yphal *w*all *p*rotein 1) is an attractive candidate for studying morphology-specific gene regulation since it is abundantly expressed in hyphal growth mode and is barely detectable in the yeast morphology (73, 74). Pseudohyphae vary in the level of *HWP1* gene expression (71). *HWP1* encodes a glycosylphosphatidylinositol-linked cell wall protein that serves as a transglutaminase substrate and enables *C. albicans* to form covalent attachments to epithelial cells that line the buccal mucosa (73, 74). Recent findings have demonstrated the presence of a critical region of the *HWP1* promoter that specifically confers developmental regulation and possesses distinct sets of protein/DNA interactions that are dependent on the morphology of the cell (29).

The regulation of *HWP1* gene expression appears to be multifaceted and involves the Cph2/Tec1, Ras/cyclic AMP (cAMP), Bcr1/biofilm, and mitogen-activated protein kinase signal transduction pathways to various extents depending on growth medium (38, 39, 56, 69). A number of transcriptional activators, including Cph1, Efg1, Tec1, Bcr1, and Flo8, and transcriptional repressors, such as Nrg1 and Tup1, have been shown to be critical to both hypha-specific gene expression and hyphal development (11, 27, 54, 56, 64, 69, 79). With the exception of *BCR1* (56), the null mutant phenotypes for these factors include aberrant growth morphologies in standard hyphal or yeast growth conditions, leaving open the possibility that the observed phenotype of each null mutant may be indirectly mediated through unrecognized factors that accompany morphogenesis. These findings prompt the need for experiments to investigate the possibility of a direct relationship between the structural changes in cell shape that occur during morphogenesis and *HWP1* gene expression.

Polarization of cell growth and alterations to cytoskeletal dynamics are both highly regulated during morphogenesis. Recent work has shown that the Rho-like GTPase Cdc42 plays a central role in polarization and that *C. albicans* strains deficient for wild-type *CDC42* are defective in the bud-hypha transition (50, 77). Strains carrying specific Cdc42 alterations in residue 26, 100, or 158 have revealed roles for *CDC42* in both bud-hypha transitioning and hypha-specific gene expression (78). In terms of the actin cytoskeleton, yeast growth is characterized by a uniform cortical distribution of F-actin patches and cables, as shown by staining with rhodamine-conjugated

* Corresponding author. Mailing address: Dartmouth Medical School, Vail Building, HB7550, Hanover, NH 03755. Phone: (603) 650-1629. Fax: (603) 650-1318. E-mail: Paula.R.Sundstrom@Dartmouth.edu.

† Supplemental material for this article may be found at http://ec.asm.org/.

▽ Published ahead of print on 22 August 2007.

TABLE 1. Strains used in this study

Strain	Genotype	Source or reference
SC5314	Wild type	19
CAI4	Δ*ura3*::*imm434*/Δ*ura3*::*imm434*	17
HB-12	As CAI4, but with plasmid p1902GFP integrated at the *HWP1* locus	29
E-15	As CAI4, but with plasmid pENO1GFP3 integrated at the *ENO1* locus	72
CKFY254	Δ*pfy1*::*HIS3*/Δ*pfy1*::*HIS3*	P. Chua, Cytokinetics, Inc.
CKFY354	Δ*bnr1*::*URA3*/Δ*bnr1*::*URA3*	P. Chua, Cytokinetics, Inc.
MWY1	As SC5314, but Δ*bni1*::*FRT*/Δ*bni1*::*NAT1*	This study
SMC7A/-7B	*cdc42-1*::*FRT*/*cdc42-2*::*FRT ACT1*/*act1*::*FRT-CDC42-MPAR-FRT sap2-1*::P*SAP2-1-ecaFLP*/*SAP2-2*	50
SMC8A	*cdc42-1*::*FRT*/*CDC42-2 ACT1*/*act1*::*FRT-CDC42-MPAR-FRT sap2-1*::P*SAP2-1-ecaFLP*/*SAP2-2*	50
AV03	Δ*ura3*/Δ*ura3 cdc42*::*hisG*/*cdc42-E100G*::*URA3*	78
EPDE2-3	As CAI4, but Δ*eno1*::*ENOp-PDE2-URA3*/*ENO1*	6
MWY2	As SC5314, but Δ*mea1*::*FRT*/Δ*mea1*::*NAT1*	This study
MWY3	As SC5314, but Δ*srv2*::*FRT*/Δ*srv2*::*NAT1*	This study

phalloidin, whereas hyphal cells concentrate F-actin at hyphal tips (2). Extensive work with the budding yeast *Saccharomyces cerevisiae* has shown that actin structures nucleated by Arp2/3 and the formins, Bni1 and Bnr1, form extensive branched networks and linear filaments, respectively, and similar findings have been reported for yeast forms of *C. albicans* as well (15, 41, 46). These nucleators facilitate the localized rapid polymerization of F-actin, which allows for a high degree of regulation in the generation of new actin filaments at specific locations in the cell in response to the changing environment (52). The importance of actin cytoskeletal structure and dynamics to morphogenesis is shown by experiments in which treatment of *C. albicans* cells with the microfilament destabilizer cytochalasin A prior to growth in hypha-inducing conditions results in the complete abrogation of hyphal development while preserving cellular growth processes (1).

To better understand the regulatory connections that exist between the cytoskeletal and membrane rearrangements of the *C. albicans* bud-hypha transition and hypha-specific gene expression, we have utilized chemical-genetic and genetic approaches to analyze *HWP1* expression in strains carrying a green fluorescent protein (GFP) reporter gene. Our findings reveal a coupling between the stability of the actin cytoskeleton and the up-regulation of *HWP1* gene expression and suggest a new model for *HWP1* regulation in which actin dynamics play a critical role in hypha-specific gene regulation at the *C. albicans* bud-hypha transition.

MATERIALS AND METHODS

Strains used and growth conditions. *Candida albicans* was used for all experiments (Table 1). Assessments of *HWP1* gene expression in a wild-type genetic background were conducted with *C. albicans* strain HB-12 (29) in which p1902GFP3, a *URA3*-marked plasmid containing the complete *HWP1* promoter driving GFP expression, was linearized with ClaI and integrated into the *HWP1* locus of CAI4. To generate hyphae, HB-12 cells were grown for 48 h to saturation in yeast nitrogen base minimal medium. From this saturated culture, 2.5×10^7 cells were inoculated into 5 ml of prewarmed Medium 199 (Invitrogen, Carlsbad, CA) or 5 ml of yeast extract-peptone-dextrose (YPD) medium with 10% bovine calf serum (BCS) at 37°C with shaking at 100 rpm for 3 h. For yeast-inducing conditions, the same medium conditions were used but the cells were incubated at 30°C with shaking at 250 rpm for 3 h. In both cases, cells were centrifuged at 4,000 rpm for 5 min following the induction period and washed twice with phosphate-buffered saline (PBS) prior to immediate observation.

Strains CKFY254 and CKFY354 have deletions of *PFY1* and *BNR1*, respectively, and are a gift from Penelope Chua (Cytokinetics, Inc., South San Francisco, CA). Strain SMC7A contains a conditional deletion of *CDC42*, whereas strain SMC8A retains a copy of *CDC42* and therefore serves as a control (50). Strain AV03 contains one copy of *CDC42*, whose product has a glutamic acid-to-glycine alteration at residue 100.

Nourseothricin (Werner Bioagents, Jena, Germany) was utilized for selection in YPD medium at a concentration of 450 μg/ml.

Drug treatments. The drug concentrations used for the Medium 199 experiments were as follows: cytochalasin A (Sigma-Aldrich, St. Louis, MO), 1 to 10 μg/ml; latrunculin A (Invitrogen, Carlsbad, CA), 10 to 50 μg/ml; jasplakinolide (Invitrogen, Carlsbad, CA), 1 to 20 μg/ml; benomyl (Sigma-Aldrich, St. Louis, MO), 2.5 to 50 μg/ml; propranolol (Sigma-Aldrich, St. Louis, MO), 125 to 175 μg/ml in accordance with previous work (8); brefeldin A (Sigma-Aldrich, St. Louis, MO), 10 to 50 μg/ml; ML-7 (Sigma-Aldrich, St. Louis, MO), 10 to 50 μg/ml. Drugs were dissolved in dimethyl sulfoxide as a concentrated stock solution and were added to Medium 199 or YPD plus 10% BCS at the appropriate concentration immediately before the addition of HB-12 cells.

Three methods were used to ensure that drug treatments did not compromise viability. First, methylene blue (0.01%, vol/vol, in PBS) staining revealed that a minimum of 80% of the cells survived each treatment. Second, *C. albicans* strain E-15, in which the constitutively active enolase promoter drives GFP expression (72), was exposed to the maximum utilized concentration of each drug. GFP fluorescence did not decrease after overnight exposure of E-15 to each drug under hypha-inducing conditions. Since the estimated half-life of GFP protein in yeast is approximately 7 h (47), the retention of GFP fluorescence was indicative of the continued activity of essential cellular processes following drug treatment. Third, 5×10^6 HB-12 cells were grown in Medium 199 with 10 μg/ml of cytochalasin A, latrunculin A, or jasplakinolide for 3 h at 37°C and 250-rpm shaking. Following this incubation, the cells were washed twice and resuspended in 10 μl PBS. The cells were diluted five times at a 1:10 ratio, and all six dilutions for each treatment were spotted onto a YPD plate. We found no difference in growth rates among any of the drug-treated cells in comparison to untreated control cells (data not shown).

The drug-induced effects were not growth medium dependent. Similar effects were observed when a different growth medium (YPD plus 10% BCS) was used. However, higher drug concentrations were required in media containing YPD plus 10% BCS, most likely because of the enhanced growth capacity in nutritionally richer media (24, 54). Since similar results were found with both growth media, only the results using Medium 199 are reported.

Assessment of *HWP1* gene expression by fluorescence microscopy and fluorometry. Samples were processed for epifluorescence microscopy as previously described (75). Fluorescent images were visualized with a BX-60 microscope (Olympus, Center Valley, PA) using 600× magnification and a GFP filter with 470- to 490-nm excitation and 515- to 550-nm emission. Photomicrographs of cells expressing GFP were taken using a 7.6-second exposure with an Olympus MagnaFire camera and processed using MagnaFire version 2.1 (Optronics, Inc., Goleta, CA) and Image-Pro Plus version 4.1 (Media Cybernetics, Inc., Silver Spring, MD) software. The selected images represented the appearance of the majority of cells in a given population.

Quantitation of fluorescence was performed using a Wallac 1420 Victor2 plate reader (PerkinElmer, Inc., Wellesley, MA). After incubation and washing as described above, 1.25×10^7 cells in 100 μl PBS were resuspended and trans-

TABLE 2. Oligonucleotides

Name	Sequence[a] (5′–3′)	Site added
BNI128N for	CCC**GGTACC**TTGTGCCAGAAGAATACGCCAAAGTATTAATGTCA	KpnI
BNI128N rev	CCT**GGGCCC**TTTTTTTCGTGTGATAATTCTTGGTGATAATAA	ApaI
BNI128C for	CCT**CCGCGG**TTGGTGGTGTTATGGATTCATTATTACAGAGGTTG	SacII
BNI128C rev	CCT**GAGCTC**TTTCTCTGGATCTTCTACATTACTGAAATC	SacI
BNI518N for	GGT**GGTACC**TTGTATCACAAACATCTTTTCATCATCCACTACTA	KpnI
BNI518N rev	GGT**GGGCCC**GGTTCTTTTATTTATTTATTTTTT	ApaI
BNI518C for	GGT**CCGCGG**GGTAAGCACTTTTTTTTGTATATGTATTTAAATGA	SacII
BNI518C rev	GGT**GAGCTC**GGTTGTTATCACTAAATAAACCAAAATTTGAATAC	SacI
NAT1 for	TTC**GAGCTC**GTTTAAACGTCGACACTGGATGG	SacI
NAT1 rev	CAGTAGCGCC**AGCGGAAGAGC**AACGGGATATCAAGCTTGCCTCGTCCC	SapI
MEA366 for	CCC**GGTACC**CACGCACTAACACTTAAACACACGCCC	KpnI
MEA366 rev	AGG**GGATCC**GTACAAGACGTCCAGGTGATAGATTAT	BamHI
MEA500N for	GGT**GGTACC**TTTTAATAGTATTGAGTTATCCAAGAGAGTAGTGA	KpnI
MEA500N rev	CCG**GGGCCC**AAGTTATGAAGGTATCCGTTTTTATGTCCAATAGA	ApaI
MEA500C for	GGT**CCGCGG**GTGAATTTGGTTTATTATAGTTTTGGTTTGATTCT	SacII
MEA500C rev	GGT**GAGCTC**GGTAAATCAAAATATGTTGGTTCTGGTG	SacI
MEA700N for	GGT**GGTACC**TTTCGCACTAACACTTAAACACACGCCCAT	KpnI
MEA700N rev	GGT**GGGCCC**GTACTTTTTGGTTGTTACTATATGTAAT	ApaI
MEA700C for	GGT**CCGCGG**GGTACTAGGGGTATAATACTTACTTTCTTCAACTT	SacII
MEA700C rev	GGT**GAGCTC**GGTGAATATTTGGATCAATAGCCATTGGATTA	SacI

[a] Engineered restriction sites are in boldface.

ferred to a Falcon Microtest 96-well plate (Becton Dickinson Labware, Franklin Lakes, NJ). Assays were performed in duplicate. Four separate readings for optical density (OD) at 600 nm and fluorescence (485-nm excitation and 535-nm emission) were collected for each sample. Normalization of fluorescence data with respect to cell density was accomplished by dividing the fluorescence value by the optical density for each individual reading.

Indirect immunofluorescence assay to detect Hwp1 and rhodamine-phalloidin staining to detect actin. To examine Hwp1 localization, *C. albicans* cells grown in hypha-inducing conditions were washed twice in ice-cold PBS and resuspended to a concentration of 3×10^7 cells/ml. A 200-μl sample of this resuspension was placed in an Eppendorf tube, and anti-Hwp1 antibody was added at a 1:200 dilution. The cells were incubated at 37°C for 30 min with gentle shaking, washed three times, and resuspended in 200 μl of ice-cold PBS. Alexa Fluor 488 goat anti-rabbit antibody (Molecular Probes, Eugene, OR) was then added at a 1:50 dilution, and the cells were incubated for 30 min at 37°C with gentle shaking. After three additional washes and resuspensions in ice-cold PBS, slides were prepared and visualized using the procedures described above for fluorescence microscopy (75). Images were taken using a 1.2-second exposure.

Actin structures were visualized using rhodamine-phalloidin staining, which was performed as previously described (57) using a rhodamine filter set (510- to 550-nm excitation, 570- to 590-nm emission) and a 2.4-second exposure.

Quantitation of F-actin aggregates. The total level of F-actin at the early stages of yeast and hypha development was determined using ImageJ 1.38x software (NIH, Bethesda, MD) in the manner previously described (28). Ten yeast and hyphal cells were analyzed for each individual time point and statistically analyzed as described below.

Disruption of the *C. albicans BNI1* gene. The *BNI1* knockout strain MWY1 was constructed using a *NAT1* flipper cassette that conferred resistance to nourseothricin. Upstream and downstream regions (300 base pairs in length) of genomic DNA relative to the *BNI1* coding region were amplified using primer sets BNI128N and BNI128C, respectively (Table 2), and genomic DNA as the template. The upstream region PCR product and pJK863, containing the *NAT1* flipper cassette (70), were digested with KpnI and ApaI and gel purified (QIAGEN, Valencia, CA). After treatment of the vector with calf intestinal alkaline phosphatase (Fisher Scientific, Pittsburgh, PA), the two fragments were joined using T4 DNA ligase (Invitrogen, Carlsbad, CA) and transformed into TOP10 *Escherichia coli* cells (Invitrogen, Carlsbad, CA). Plasmid DNA was purified from transformants and verified by DNA sequencing. The PCR product corresponding to the region downstream of the *BNI1* open reading frame and the plasmid containing the upstream region were digested with SacI and SacII prior to ligation and were transformed into TOP10 *E. coli* cells as described above.

The resultant *BNI1* deletion cassette, pBNIDEL128, was digested with KpnI and SacI to release the 4.2-kb flipper cassette and *BNI1* flanking regions. The cassette was recovered by gel extraction and used for electroporation of strain SC5314 (63). Transformants were selected on YPD plates with nourseothricin and verified by Southern blotting using EcoRV digestion and a PCR-amplified complete genomic copy of *BNI1* as the probe (not shown).

A nourseothricin-sensitive *BNI1*/*bni1*Δ strain was created by excision of the *NAT1* cassette using standard techniques (70). Excision of the *NAT1* cassette was confirmed by Southern blotting using EcoRV digestion and a PCR-amplified complete genomic copy of *BNI1* as the probe (not shown).

For the second round of *BNI1* deletion, oligonucleotides that were slightly displaced from the genomic location of the original deletion to prevent recombination between the new flipper cassette and the regions flanking the excised copy of *BNI1* were designed. A PCR using primer set BNI518N generated the KpnI-ApaI upstream fragment of *BNI1*, whereas primer set BNI518C generated the SacII-SacI downstream fragment of *BNI1*. Ligation of these two fragments to the ends of the *NAT1* flipper cassette generated plasmid pBNIDEL518. Deletion of the second copy of *BNI1* was performed as described above.

Cloning and disruption of *C. albicans MEA1*. The *Aspergillus nidulans* MesA amino acid sequence (60) was used as a query to search the predicted open reading frames in the *C. albicans* genome (4) using BLASTP, leading to the identification of ORF19.5919. Global alignment using Enboss Needle at EMBL-EBI (http://ebi.ac.uk) showed 57.4% similarity and 20.7% identity between the two sequences. In four previously identified conserved regions (60), homology was as high as 65% similarity and 47% identity (see Fig. S1 in the supplemental material for complete alignment analysis). The gene containing ORF19.5919 was named *MEsA1* or *MEA1*. A 2,482-bp DNA segment containing *MEA1* was synthesized by PCR using primer set MEA366 and genomic DNA as the template. This PCR product, which included 303 bp of upstream flanking sequence, 1,879 bp of coding sequence, and 300 bp of downstream flanking sequence, was sequenced and cloned into the pBluescript SK(−) vector to generate pBSMEA366. The *MEA1* deletion strain MWY2 was generated in the manner described above for the deletion of *BNI1*. Primer sets MEA500N and MEA500C were utilized to generate *MEA1* flanking regions for ligation to the *NAT1* flipper cassette and deletion of the first copy of *MEA1*, whereas primer sets MEA700N and MEA700C were used for deletion of the second copy. pBSMEA366 was used as template for the PCRs.

Insertion of the *HWP1* reporter plasmid into *bni1*Δ/*bni1*Δ, *bnr1*Δ/*bnr1*Δ, and *pfy1*Δ/*pfy1*Δ deletion strains and Cdc42 point mutant strain AV03. The nourseothricin resistance marker was inserted into p1902GFP3 prior to transformation into the *bni1*Δ/*bni1*Δ, *bnr1*Δ/*bnr1*Δ, and *pfy1*Δ/*pfy1*Δ deletion strains as well as the Cdc42 point mutant strain AV03. Plasmid JK795 (70), containing the complete *NAT1* genomic region, was used as the template for primer set NAT1. The resulting PCR-amplified fragment contained the complete *NAT1* genomic region flanked by SacI and SapI restriction sites at its 5′ and 3′ ends, respectively. This fragment and p1902GFP3 were both digested with SacI and SapI and ligated together to generate p1902GFP3NAT1, an *HWP1* reporter plasmid that contains *URA3* and *NAT1* markers on opposite sides of *HWP1*-driven GFP. This plasmid was targeted to the enolase locus of each *C. albicans* strain of interest following

ClaI linearization. Each strain was transformed via electroporation, selected on YPD plates containing nourseothricin, and verified via Southern blotting using BglII digestion and genomic enolase as a probe to recognize corresponding sequences present in p1902GFP3NAT1 (not shown).

Examination of *HWP1* gene expression in the *CDC42* inducible deletion strain. The p1902GFP3NAT1 plasmid was transformed by electroporation into SMC7A and SMC8A (50) using the above methods. Transformants were selected on YPD plates containing nourseothricin and confirmed by Southern blotting using BglII digestion and genomic enolase as a probe (29) (not shown). Overnight growth in yeast carbon base-bovine serum albumin media led to the excision of the ectopic copy of *CDC42* in SMC7A localized to the *ACT1* locus in the manner previously described for excision of the *BNI1* flipper cassette to create a *cdc42*Δ/*cdc42*Δ strain. Analysis of the induced *cdc42*Δ/*cdc42*Δ strain was carried out under hypha-inducing conditions as described above.

Kinetic analysis of *HWP1* gene expression. To examine *HWP1* gene expression and actin structures during the development of yeast buds and hyphal germ tubes, strain HB-12 was grown under yeast- and hypha-inducing conditions as described above. Cell samples were taken at 15-min intervals over a 120-min period and examined for morphology, *HWP1* gene expression, and actin by differential interference contrast (DIC) and epifluorescence microscopy. To quantitate *HWP1* up-regulation rates, strain HB-12 with or without 1, 5, or 10 μg/ml cytochalasin A or 10 μg/ml jasplakinolide was analyzed every 10 min over a 150-min period by fluorometry. Strains MWY1 and AV03 were analyzed in a similar manner. Experiments were performed in triplicate.

Addition of exogenous cAMP to actin-deficient cells. Strain HB-12 was induced to form hyphae in the presence or absence of 5 μg/ml or 10 μg/ml cytochalasin A and 10 mM dibutyryl-cAMP (Roche Diagnostics, Basel, Switzerland). Measurements were taken every 30 min over a 150-minute time period. Strain MWY3 was analyzed in a similar manner. Experiments were performed in triplicate and statistically analyzed as described below.

cAMP assay. Intracellular cAMP in Medium 199 was extracted as previously described (16) and measured using the cAMP Biotrak enzyme immunoassay system according to the manufacturer's instructions (GE Healthcare, Piscataway, NJ). Cells were prepared for hypha formation in the manner described above, and samples were taken at 30-minute intervals over a 120-min time period. Experiments were performed in triplicate and statistically analyzed as described below.

Statistical analysis. Unless otherwise indicated, statistical analysis was performed using the one-way analysis of variance and Bonferroni's multiple-comparison test performed with Prism 4.03 software (GraphPad, San Diego, CA).

RESULTS

Assessment of *HWP1* gene expression in the presence of drugs that interfere with *Candida albicans* hypha formation. A chemical-genetic approach was initially utilized to assess the relationship between *HWP1* gene expression and hyphal morphogenesis. These experiments were performed using *C. albicans* strain HB-12 (29), in which the *HWP1* coding region was replaced by yEGFP3, leading to the presence of GFP throughout the cytoplasm of cells under germ tube-inducing conditions but not yeast-inducing conditions (Fig. 1A). If the formation of true hyphae were necessary for *HWP1* expression, then cells in which hypha formation was blocked by drug treatment would also be unable to activate *HWP1*. Conversely, *HWP1* expression during a drug-induced blockade of hypha formation could bring to light information about processes that stimulate *HWP1* gene expression independently of physical hyphal structure.

As expected given the tight coupling between *HWP1* gene expression and hyphal growth, inhibition of hypha formation using five of seven drugs tested was accompanied by the loss of *HWP1*-mediated GFP fluorescence in the majority of cells examined (Fig. 1B). Control experiments verified that these results were not caused by a loss of cellular viability (see Materials and Methods). Results using the F-actin destabilizer cytochalasin A (1) were typical of the results with other drugs, which included latrunculin A (13), benomyl (22), propranolol, (8), and ML-7 (45), that indicated loss of both *HWP1* gene expression and hypha formation (Fig. 1A).

By contrast, abrogation of hypha formation by the F-actin stabilizer jasplakinolide (10, 68) and the reversible disruptor of Golgi complex-mediated secretion brefeldin A (43) was not accompanied by the abolition of *HWP1* gene expression in ~90% of cells (Fig. 1C). Experiments using *S. cerevisiae* have shown that jasplakinolide causes the formation of actin clumps that are extremely stable, cannot be dispersed by the monomer sequestering agent latrunculin A, and are therefore not dynamic (5). Nonetheless, the actin structures stabilized by jasplakinolide are structurally and functionally similar to normal F-actin in that they continue to associate with proteins that normally associate with F-actin and bind anti-actin antibodies (5). As expected, stabilized actin clumps were observed in *C. albicans* treated with jasplakinolide when detected with rhodamine-conjugated phalloidin (Fig. 2A).

Despite the blockage in hypha formation in jasplakinolide- and brefeldin A-treated cells, hypha-inducing conditions were required for *HWP1* expression. Fluorescence reflecting *HWP1* gene expression was not detected in yeast growth conditions upon treatment with jasplakinolide or brefeldin A (Fig. 2B, results with jasplakinolide). These results suggested that signal transduction pathways that relay environmental conditions favoring *HWP1* expression were not interrupted by treatment with jasplakinolide or brefeldin A whereas the opposite was true for cytochalasin A and the other drugs described above.

Detection of Hwp1 on drug-treated cells using indirect immunofluorescence. To determine if Hwp1 protein was detectable on cell surfaces, drug-treated cells of strain HB-12 were examined for the presence of Hwp1 protein by the indirect immunofluorescence assay using monospecific anti-Hwp1 antibody. Hwp1 was found exclusively on the surfaces of hyphae in almost all untreated cells (Fig. 3, panel 2) and at discrete regions on the surfaces of the vast majority of cells treated with jasplakinolide or brefeldin A despite the lack of a discernible hyphal structure (Fig. 3, panels 6, 8, and 10). In the case of jasplakinolide-treated cells, multiple polarization sites containing Hwp1 could be detected, suggesting a loss in the ability to organize and commit to a single site of hypha emergence.

Hwp1 was also clearly present in discrete surface aggregates on ~50% of cells that were blocked in hypha formation by cytochalasin A (Fig. 3, panel 4). Although GFP reflecting *HWP1* gene expression was not evident in the merged epifluorescence and DIC image (Fig. 3, panel 3), GFP was detectable at a low level in the dark-field fluorescent image of cytochalasin A-blocked cells compared to yeast form cells (compare Fig. 1B, panel 6, and 1A, panel 2). Similar results were also found for latrunculin A-treated cells (not shown). In both cases, the majority of cells that showed the presence of Hwp1 patches had a slightly oval or pear-shaped appearance, a shape that is characteristic of cells immediately prior to germ tube emergence. These results showed that the processes controlling polarization of cell surface proteins in hypha-inducing conditions were retained during drug treatments that inhibited germ tube elongation and revealed the presence of a low level of *HWP1* gene expression under these conditions that was barely visible by epifluorescence microscopy to detect the GFP reporter.

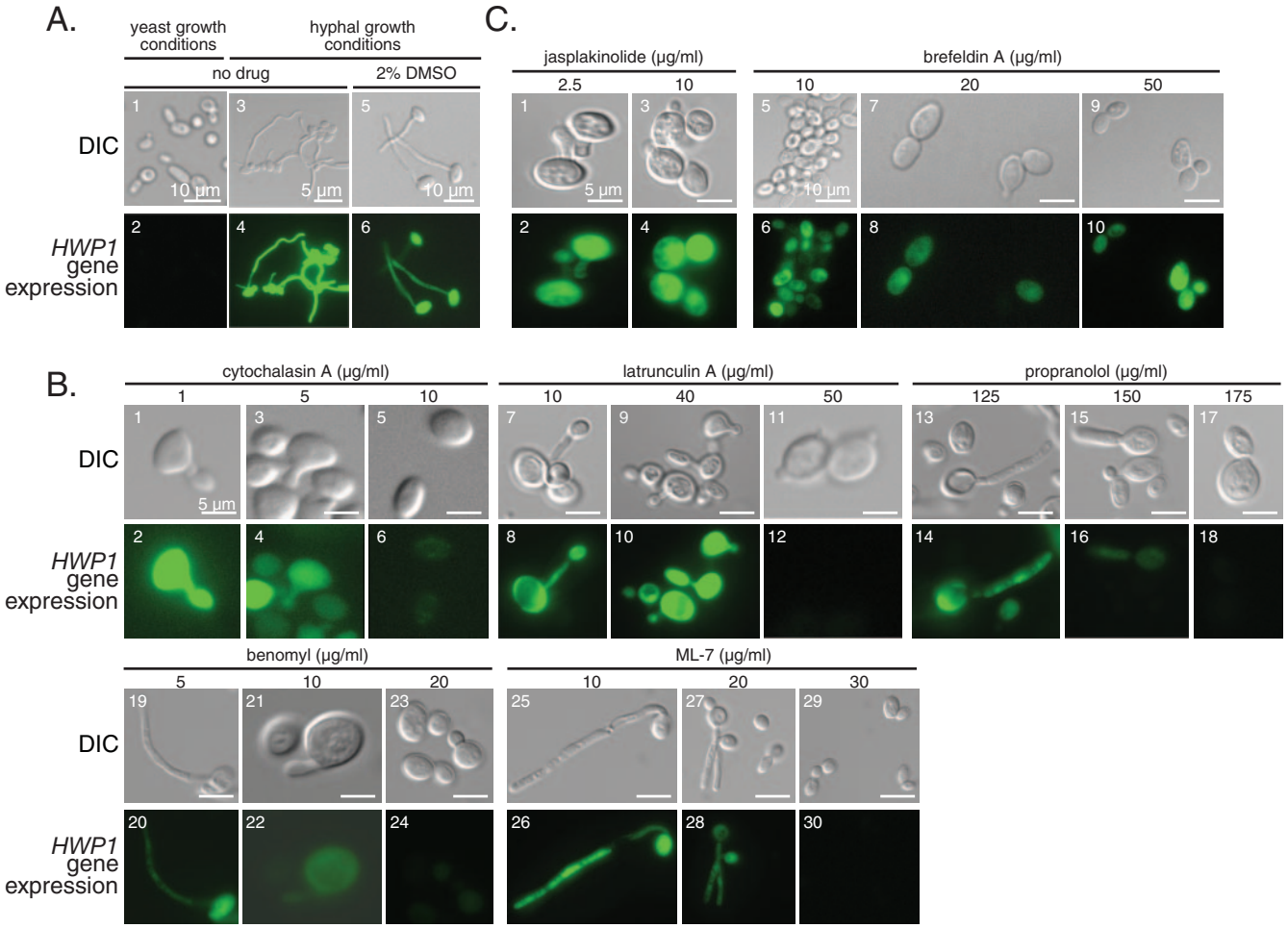

FIG. 1. *HWP1* gene expression in the presence of drug treatments to disrupt hyphal morphology. (A) *C. albicans* strain HB-12, containing GFP under the control of the *HWP1* promoter, was incubated in conditions supporting yeast (1 and 2) or hyphal (3 to 6) growth. The addition of 2% dimethyl sulfoxide (5 and 6) had no effect on hypha formation or GFP fluorescence. (B) Drug treatments that disrupted hyphal growth with loss of *HWP1* gene expression: cytochalasin A (1 to 6), latrunculin A (7 to 12), propranolol (13 to 18), benomyl (19 to 24), and ML-7 (25 to 30). (C) Drug treatments that preserved *HWP1* gene expression despite the loss of hypha formation included jasplakinolide (1 to 4) and brefeldin A (5 to 10). Note that fluorescence reflecting *HWP1* gene expression upon loss of hyphal morphology is intense with jasplakinolide at 10 μg/ml and is barely detectable with cytochalasin A at 10 μg/ml in the dark-field image (B, 6). DIC microscopy (odd-numbered panels) and epifluorescence microscopy (even-numbered panels) were used to detect morphology and *HWP1* gene expression, respectively. Drugs were used at the indicated concentrations.

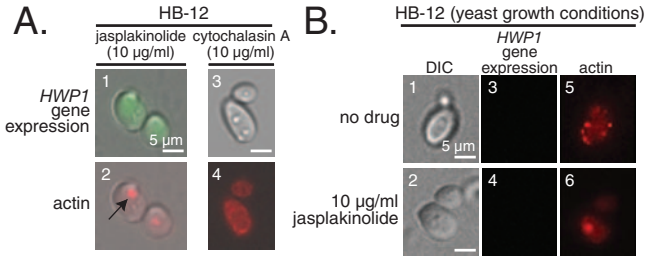

FIG. 2. (A) Correlation between *HWP1* gene expression and the presence of aggregated actin structures in strain HB-12 treated with 10 μg/ml cytochalasin A or jasplakinolide under hypha-inducing conditions. F-actin was detected by staining with rhodamine-conjugated phalloidin. F-actin was aggregated following treatment with 10 μg/ml jasplakinolide (2, arrow) but not with 10 μg/ml cytochalasin A (4). GFP fluorescence reflecting *HWP1* gene expression was observed in the presence of jasplakinolide (1) but not cytochalasin A (3). (B) *HWP1* gene expression was absent in cells grown under yeast conditions in the presence or absence of 10 μg/ml jasplakinolide.

Reduced *HWP1* gene expression in mutants defective in F-actin nucleation. The opposite effects of jasplakinolide treatment versus cytochalasin A or latrunculin A treatment on *HWP1* gene expression as assessed by measuring GFP production pointed to the possibility that actin dynamics plays a pivotal role in *HWP1* expression. The observation that cells treated with jasplakinolide, which stabilizes actin and promotes the formation of polymeric actin structures (5), retained *HWP1* gene expression despite the lack of true hyphal development suggested that F-actin in cells undergoing bud-hypha transitions may be important for the up-regulation of *HWP1*. To obtain genetic evidence in support of this hypothesis, mutants with defects in actin cable nucleation were analyzed for the presence of reduced *HWP1* gene expression.

Previous work with *S. cerevisiae* and *C. albicans* has demonstrated the importance of the formin gene *BNI1* for efficient actin cable formation and for *C. albicans* hyphal development

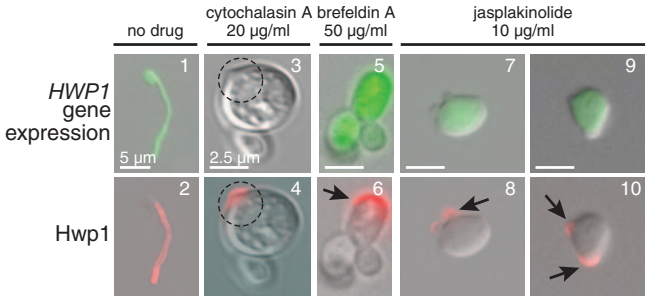

FIG. 3. Hwp1 localization in the presence of disrupted hyphal morphology. Hwp1 was detected on hyphal cell surfaces of strain HB-12 in the absence (1 and 2) or presence of cytochalasin A (3 and 4), brefeldin A (5 and 6), or jasplakinolide (7 through 10) by indirect immunofluorescence using anti-Hwp1 primary antibody and Texas Red-conjugated goat anti-rabbit secondary antibody. Drugs were used at the indicated concentrations. Fluorescence produced by the GFP reporter reflected *HWP1* gene expression. Note the putative site of germ tube formation (3, dashed circle) and the aggregation of Hwp1 in this region (4, dashed circle) in the cytochalasin A-treated cell, in which *HWP1* gene expression, as assessed by measuring the fluorescence of GFP, was not detectable. Hwp1 was confined to localized regions of the cell surface of brefeldin A (6, arrow)- and jasplakinolide (8 and 10, arrows)-treated cells. Images 3 to 10 are shown at the same scale as image 3.

(15, 41, 46). Therefore, a *bni1*Δ/*bni1*Δ mutant strain (MWY1) containing p1902GFP3NAT1 was created. Upon growth under hypha-inducing conditions, the majority of MWY1 cells produced hyphae that were wider and less consistent in width than wild-type hyphae (Fig. 4A). MWY1 also showed a reduction in *HWP1* gene expression, which was 63% of control levels as detected by fluorometry (Fig. 4A and C). Identical results were obtained using a *bni1*Δ/*bni1*Δ strain produced in Yue Wang's laboratory (Institute of Molecular and Cell Biology, Singapore) (41).

Additional genetic data regarding the relationship between hyphal morphogenesis and *HWP1* gene expression were acquired using strain AV03, which contains a Cdc42 glutamic acid-to-glycine alteration at residue 100 (78). The analogous residue in *S. cerevisiae* Cdc42 is critical for activating Bni1 and for formin-mediated actin assembly at sites of bud emergence (14, 51, 52, 78). AV03 cells transformed with p1902GFP3NAT1 showed alterations in hyphal structures that were similar to those found for untransformed AV03 (i.e., hyphae were shorter and wider than wild type [78]) (Fig. 4B). Quantitatively, *HWP1* gene expression was present but was reduced to 47% of that seen in HB-12 under identical growth conditions (Fig. 4B and C). This reduction is similar to the 63% level seen in the *bni1*Δ/*bni1*Δ background and is consistent with the predicted effect of a loss of interaction between Cdc42 and Bni1 (Fig. 4C). The reductions in fluorescence of the *bni1*Δ/*bni1*Δ and AV03 strains transformed with p1902GFP3NAT1 compared to HB-12 were statistically significant.

The effect of the formins on *HWP1* gene expression was restricted to *BNI1*. The *bnr1*Δ/*bnr1*Δ knockout did not deviate from control cells in hypha formation or in the ability to activate *HWP1* (Fig. 4C). Likewise, the actin monomer recruiter profilin was not required. *C. albicans* profilin has been shown to be functionally similar to *S. cerevisiae* profilin (59), and the two proteins share extensive sequence homology (87% similarity, 72% identity). The *pfy1*Δ/*pfy1*Δ strain showed alterations to hyphal structure similar to those observed in the *bni1*Δ/*bni1*Δ strain (not shown); however, *HWP1* gene expression was not reduced in *pfy1*Δ/*pfy1*Δ cells (Fig. 4C).

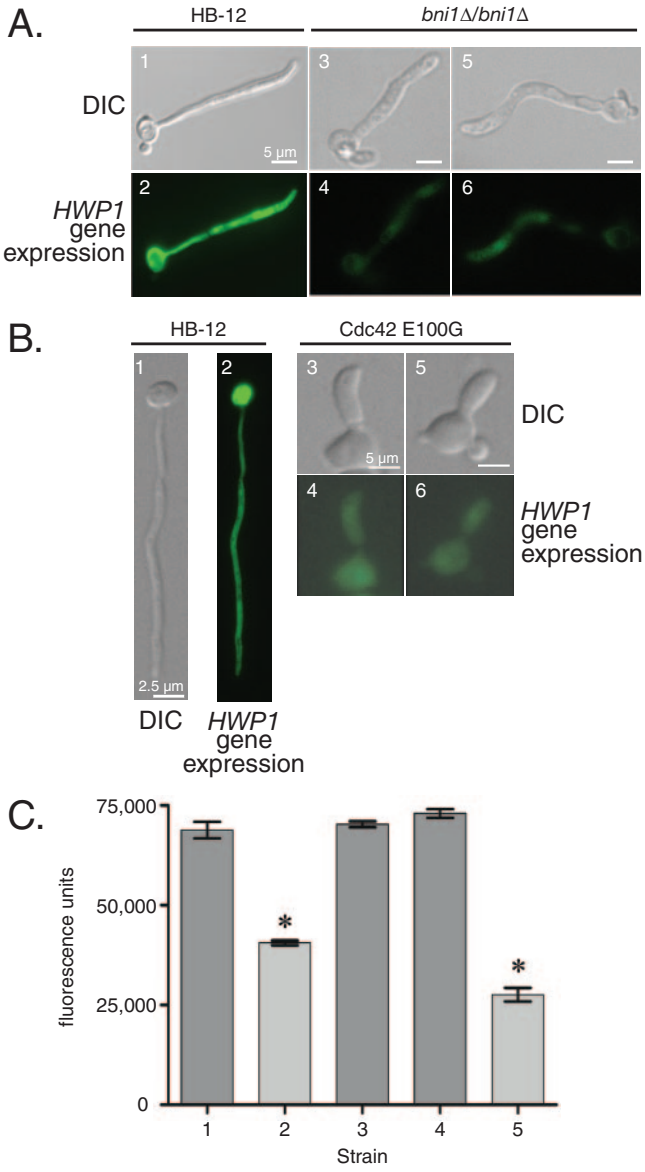

FIG. 4. *HWP1* gene expression in mutants defective for actin nucleation. *C. albicans* strains CKFY254 (*pfy1*Δ/*pfy1*Δ), CKFY 354 (*bnr1*Δ/*bnr1*Δ), MWY1 (*bni1*Δ/*bni1*Δ), and AV03 (Cdc42 E100G) were transformed with p1902GFP3NAT1 to monitor *HWP1* gene expression in comparison to strain HB-12 (A and B). Microscopic analysis of hyphae by DIC (1, 3, and 5) and epifluorescence (2, 4, and 6) microscopy was performed to detect *HWP1* gene expression in strains HB-12 and MWY1 (A) and AV03 (B). Note the decreased fluorescence of the *bni1*Δ/*bni1*Δ (A, 4 and 6) and Cdc42 E100G (B, 4 and 6) strains compared to that of HB-12 (2), an effect that was not observed in *bnr1*Δ/*bnr1*Δ and *pfy1*Δ/*pfy1*Δ cells (not shown). (C) Fluorometry to quantitate *HWP1* gene expression in the *bni1*Δ/*bni1*Δ and Cdc42 E100G strains (strains 2 and 5; light bars) and in the HB-12, *bnr1*Δ/*bnr1*Δ, and *pfy1*Δ/*pfy1*Δ strains (strains 1, 3, and 4; dark bars). *, $P < 0.001$ (*bni1*Δ/*bni1*Δ strain versus HB-12 and Cdc42 E100G strain versus HB-12).

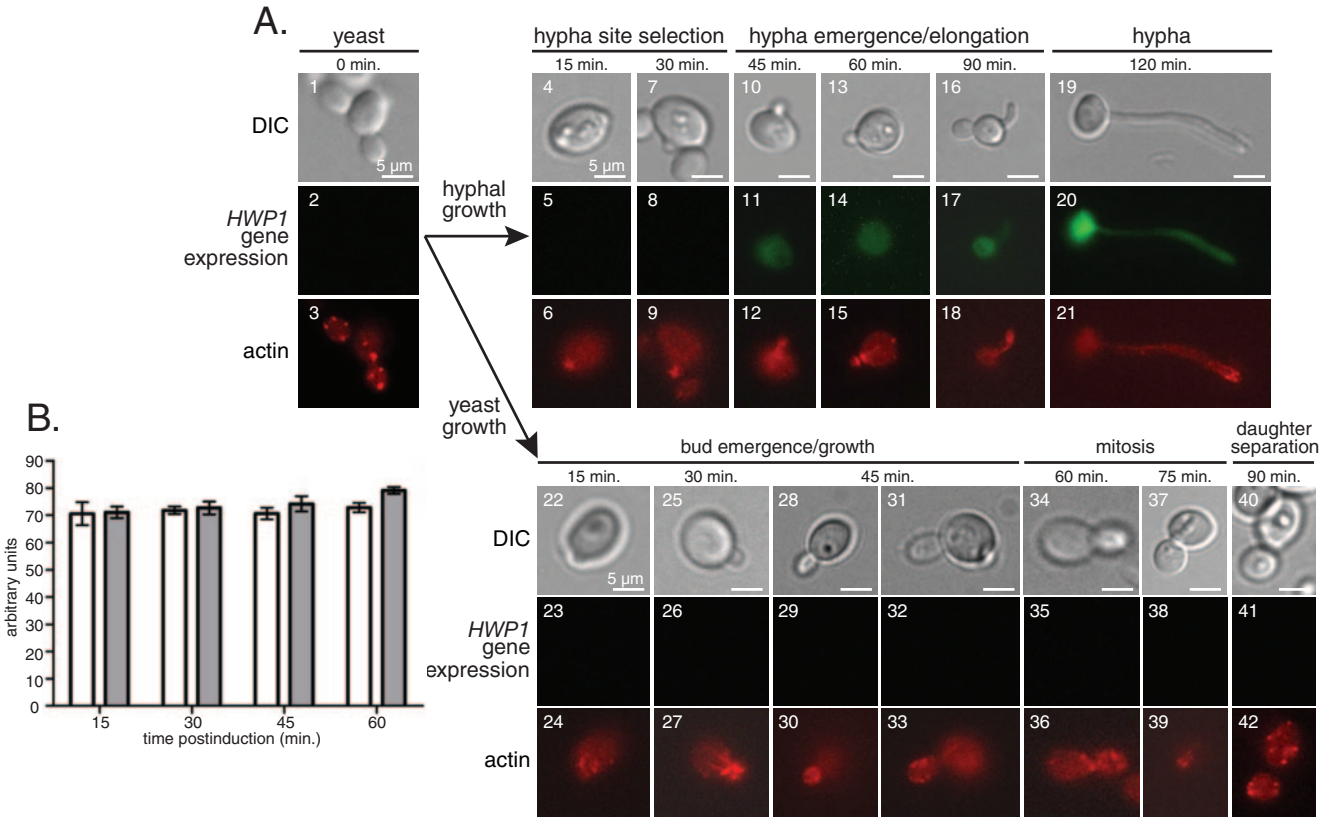

FIG. 5. (A) Correlation between hypha formation, actin polarization, and *HWP1* gene expression. Cells were grown in hypha (4 to 21)- or yeast (22 to 42)-inducing conditions and examined for morphology (top rows), *HWP1* gene expression (middle rows), and rhodamine-phalloidin stained F-actin (bottom rows). A different individual cell is shown at each time point. (B) Quantitation of F-actin prior to germ tube and bud emergence. The amount of aggregated F-actin is shown for hyphal (gray bars) and yeast (white bars) cells.

The genetic studies were consistent with the drug studies in that reduced levels of *HWP1* gene expression were found using two mutants that are deficient in F-actin nucleation.

Kinetics of expression of the *HWP1* gene relative to actin polarization. To investigate the reasons for the differences in GFP levels at 2.5 h between cells treated with jasplakinolide and those treated with cytochalasin A or latrunculin A, the kinetics of increases in GFP reporter expression over time during germ tube inducing conditions were assessed.

(i) Microscopic analysis. The actin cytoskeleton and GFP fluorescence reflecting *HWP1* gene expression were analyzed at 15-min intervals in cells grown under hypha-inducing or yeast growth conditions (Fig. 5A). In hyphal cells at 30 min postinduction, F-actin began to polarize to a site of germ tube emergence but GFP fluorescence was not observed (Fig. 5A, panels 7 to 9), confirming work from the Liu laboratory (24).

The polarization of actin to the site of the nascent germ tube occurred just before GFP fluorescence became detectable, at 45 min postinduction (Fig. 5A, compare panels 8 and 9 to panels 11 and 12). A rapid rate of increase in GFP fluorescence that was quantified by fluorometry occurred after 60 min of induction [see "Kinetics of expression of the *HWP1* gene relative to actin polarization. (iii) Slow and fast kinetics of HWP1 gene expression during hypha induction"]. By contrast, GFP fluorescence was not observed during budding and mitosis in yeast cells.

(ii) Quantitation of F-actin in yeast and hyphal growth. Previous work by Hazan et al. (24) suggested the presence of permanently polarized actin at the point of germ tube emergence that was not dispersed during the G_1 phase of the yeast cell cycle, when cell cycle-regulated actin became depolarized. This prompted questions regarding whether or not this apical F-actin constituted an absolute increase in the amount of F-actin during the emergence of germ tubes compared to that during bud emergence. To address this question, we quantified the total cellular F-actin from yeast and hyphal cells during the first 60 min of induction according to previously described procedures (28). Although a slight increase in F-actin levels in hyphal cells relative to yeast cells was observed at 60 min, this difference was not statistically significant (Fig. 5B), suggesting that the observed aggregation of F-actin to both the nascent germ tube and the nascent bud in their respective growth conditions represents a redistribution of existing cellular F-actin populations in response to polarization signals.

(iii) Slow and fast kinetics of *HWP1* gene expression during hypha induction. Previous work showed that the rate of *HWP1* gene expression increased after 60 min of induction (29). To explore the kinetics of *HWP1* expression within the first 2.5 h of induction, GFP fluorescence levels were monitored by fluorometry at 10-minute intervals. Two distinct rates of increasing fluorescence were observed; these reflected the presence of a slow phase followed by a fast phase, with average rates of

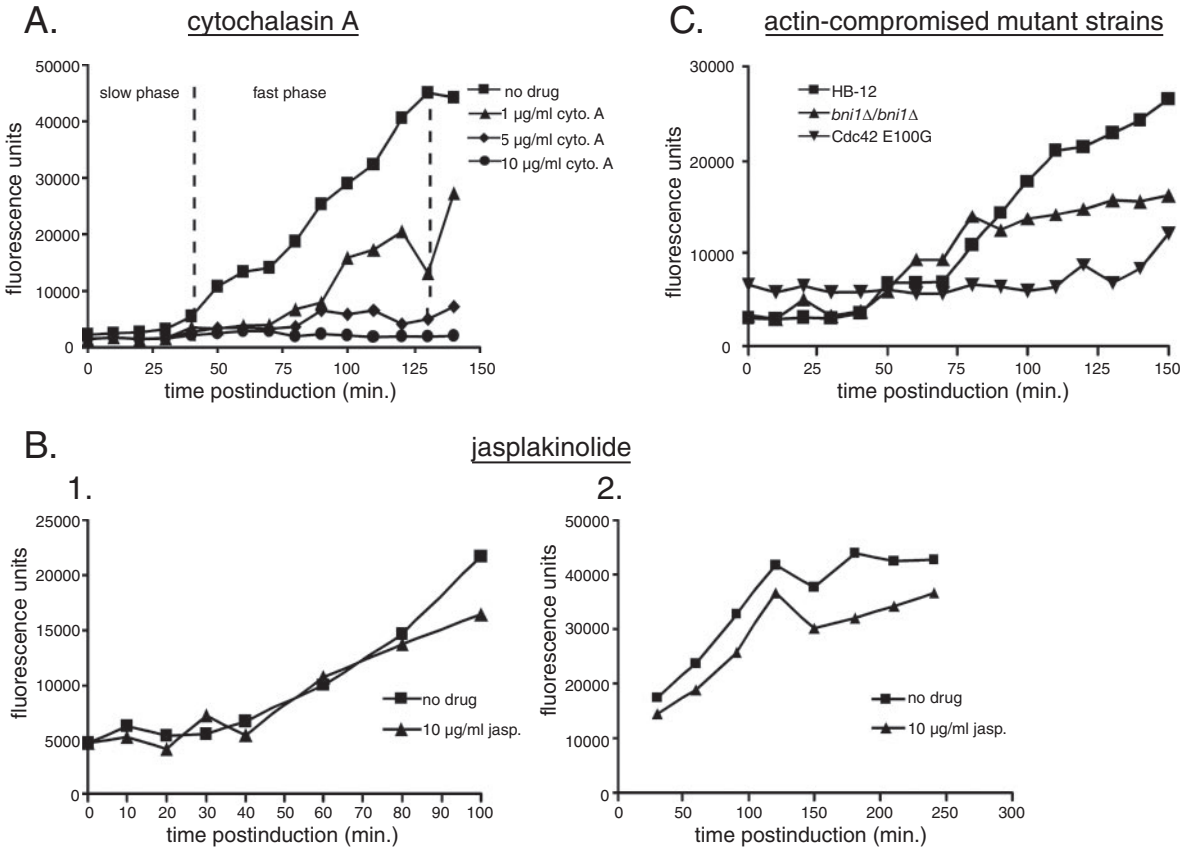

FIG. 6. Role of F-actin in the kinetics *of HWP1* gene expression. (A) Cytochalasin A (cyto. A)-treated HB-12. (B) Jasplakinolide-treated (10 μg/ml) HB-12 cells in the slow (1) or fast (2) phase of *HWP1* gene activation. (C) Strains MWY1 (*bni1*Δ/*bni1*Δ) and AV03 (Cdc42 E100G). Each graph in panels A to C is a representative example of experiments that were repeated three times.

135.7 and 362.7 fluorescence units/min, respectively (Fig. 6A). The difference between the slow and fast rates of expression was statistically significant ($P < 0.001$ using the paired Student *t* test on data from three independent experiments). The transition period at 50 to 70 min postinduction roughly correlated with both the appearance of intense actin polarization at the emerging hypha (Fig. 5A) and the spike in cAMP that naturally occurs following the shift to hypha-inducing conditions (7).

(iv) Effect of chemical or genetic interference with actin dynamics on the kinetics of *HWP1* gene expression. To further examine the role of F-actin in *HWP1* gene expression, kinetics were examined with actin-influencing drugs as well as with actin-compromised mutant strains. At concentrations of cytochalasin A that did not completely block germ tube formation (1 μg/ml), the level of *HWP1* expression in the fast phase was reduced (Fig. 6A). At concentrations of 5 μg/ml and 10 μg/ml of cytochalasin A the fast phase was blocked (Fig. 6A). By contrast, cells treated with 10 μg/ml jasplakinolide showed levels of *HWP1* gene expression that were 70% of those seen in the absence of drug with kinetics of expression that were identical to untreated cells (Fig. 6B).

The kinetics of *HWP1* gene expression were also altered in mutants with deficiencies in actin nucleation. The *bni1*Δ/*bni1*Δ and Cdc42 E100G strains showed similar kinetics to HB-12 during the slow phase of expression (Fig. 6C). Although the *bni1*Δ/*bni1*Δ strain showed an increase in *HWP1* gene expression during the fast phase, this increase was reduced relative to HB-12. The *bni1*Δ/*bni1*Δ strain appeared to enter the fast phase of *HWP1* gene expression, but the fast phase was not maintained. The Cdc42 E100G strain showed slight increases in *HWP1* expression levels that were markedly reduced in comparison to those shown by HB-12.

The results of the kinetic analysis suggested that activation of *HWP1* gene expression occurs by a two-step process consisting of a slow actin-independent phase followed by a fast F-actin-dependent phase. While GFP reporter levels reflecting *HWP1* activation are measurable by fluorometry during the slow phase of expression, it is only after 50 to 70 min of induction, when actin is polarized to the site of apical growth in the majority of cells (Fig. 5A), that rapid up-regulation of *HWP1* occurs and GFP is readily visualized by epifluorescence microscopy of single cells. Only the fast phase is disrupted by the use of chemical or genetic disruptors of F-actin, implicating F-actin as a central player in the fast phase of *HWP1* expression. Although GFP levels are slightly reduced at each time point in jasplakinolide-treated cells in the fast phase, the kinetics of the fast phase of activation are neither diminished nor enhanced by jasplakinolide, which stabilizes and extends existing filaments and causes filament nucleation de novo (68).

***HWP1* expression and localization in the absence of polarization. (i) *CDC42*.** *CDC42* is an essential gene in *S. cerevisiae*

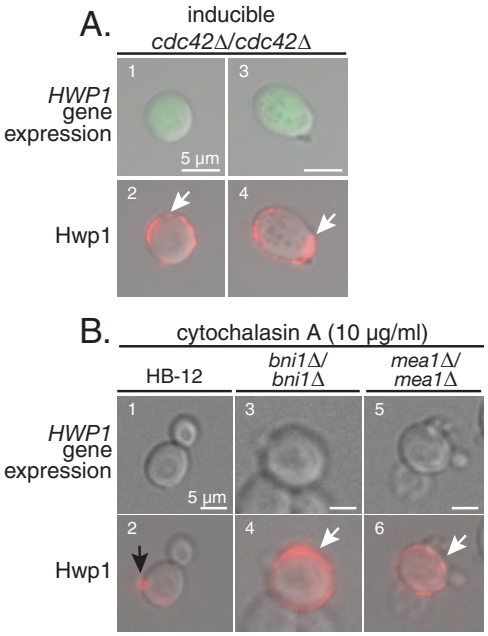

FIG. 7. Presence of *HWP1* gene expression in cells made defective for cell surface polarization using chemical and genetic methods. Interference with cell surface polarization was accomplished using SMC7A grown under conditions leading to the loss of *CDC42* (A) or using strains MWY1 (*bni1*Δ/*bni1*Δ) and MWY2 (*mea1*Δ/*mea1*Δ) that had been treated with cytochalasin A (B). Strain HB-12 served as a wild-type control. Strain HB-12 showed a punctate distribution of Hwp1 (B, 2, black arrow), in contrast to cells in which polarization was inhibited (B, 4 and 6, white arrows).

and *C. albicans* (26, 51). However, the loss of *CDC42* can be studied by using strain SMC7A, in which *CDC42* can be inducibly deleted following growth in yeast carbon base-bovine serum albumin medium and subsequent excision of an ectopic copy of *CDC42* from the genome (50). Loss of *CDC42* gave rise in most cases to large, round cells that had lost the ability to exhibit polarized growth and were terminal (Fig. 7A). Measurable GFP fluorescence was found under hypha-inducing conditions in strain SMC7A, which had been transformed with p1902GFP3NAT1, despite the inability of the cells to form true hyphae. This result added additional genetic evidence for the independence of the regulatory pathways governing the formation of true hyphal structures and *HWP1* expression. Indirect immunofluorescence assays showed that Hwp1 was present on cell surfaces but was not confined to specific areas; rather, Hwp1 was extended across the entire cell surface (Fig. 7A). Polarization of the cell surface was not required for high levels of *HWP1* expression, which could be determined by measuring GFP fluorescence.

(ii) Drug treatments of mutants with defects in polarization. The role of Bni1 in cell polarization has been previously described (14, 36). The *C. albicans MEA1* gene is similar to *MesA* of *Aspergillus nidulans*, which encodes a protein responsible for the localized assembly of actin cables at polarization sites by recruitment of the formin SepA (60) (see Fig. S1 in the supplemental material). As expected, *HWP1* gene expression was not sufficient to elicit detectable fluorescence from the GFP reporter for either mutant or for HB-12 in the presence of cytochalasin A (Fig. 7B, panels 1, 3, and 5). The low level of Hwp1 characteristic of the early stage of *HWP1* gene expression was present in both mutants as well as in HB-12; however, Hwp1 was not polarized in the mutant strains but was more evenly distributed over the cell surface. Thus, polarization events were not required for the initial low-level stage of expression of *HWP1*.

Expression of *HWP1* by stabilized actin involves the cAMP pathway. (i) Studies using cAMP hypo- and hypermorphic strains of *C. albicans*. Recent work using *S. cerevisiae* endocytosis mutants that display reduced actin dynamics and the presence of F-actin aggregates has shown that an up-regulation of the cAMP signaling pathway is associated with F-actin aggregation and that the adenylyl cyclase-associated protein, Srv2p (also called Cap1), is required for increases in cAMP (21). To investigate whether *HWP1* gene expression in the presence of stabilized actin structures was also related to activation of the cAMP pathway, GFP fluorescence and actin structures were monitored in a strain that constitutively overexpresses *PDE2* (EPDE2-3) (6), causing enhanced degradation of cAMP. The *HWP1GFP* reporter gene was introduced into strain EPDE2-3 using plasmid p1902GFPNAT1. Overexpression of *PDE2* eliminated observable GFP fluorescence among jasplakinolide-treated cells despite the presence of stabilized actin structures (Fig. 8A, panels 1 and 2). *HWP1* gene expression in the presence of jasplakinolide was also not observed in the *srv2*Δ/*srv2*Δ mutant strain, which is deficient in the activation of the cAMP pathway (7) (Fig. 8A, panels 3 and 4).

The initial stage of *HWP1* gene expression was not dependent on the cAMP signaling pathway. Surface Hwp1 as detected by indirect immunofluorescence was present in a distinct patch on surfaces of *srv2*Δ/*srv2*Δ and EPDE2-3 strains (Fig. 8B, panels 2 and 4), arguing against a role for the cAMP signaling pathway in the initial stage of *HWP1* gene expression. However, the data strongly suggest that activation of the cAMP signaling pathway is related to the expression of *HWP1* to the high levels required for detection via GFP reporter fluorescence in the presence of stabilized actin.

(ii) The effect of chemical or genetic interference with F-actin on cAMP levels. If the loss of *HWP1* gene expression in cytochalasin A- and latrunculin A-treated cells is related to reduced cAMP levels, then cells treated with these drugs should have reduced levels of cAMP compared to untreated cells. Furthermore, mutants with defects in actin nucleation should also exhibit reduced levels of cAMP. The addition of 10 μg/ml cytochalasin A to HB-12 cells reduced intracellular levels of cAMP to one-half the level seen in untreated cells following 60 min of induction, a time that coincides with the slow/fast phase transition (Fig. 8C). A gradual decline in cAMP levels followed the 60-minute time point. By contrast, latrunculin A (50 μg/ml) did not alter the peak of cAMP at 60 min; however, a reduction in intracellular cAMP to 66% of untreated-cell levels by 120 min postinduction was observed. The difference in magnitude between the cytochalasin A and latrunculin A results up to 90 min postinduction could be related to the slow monomer-sequestering mechanism by which the latter acts on actin filaments (13). Also, the disruption to the actin cytoskeleton by latrunculin A-based actin

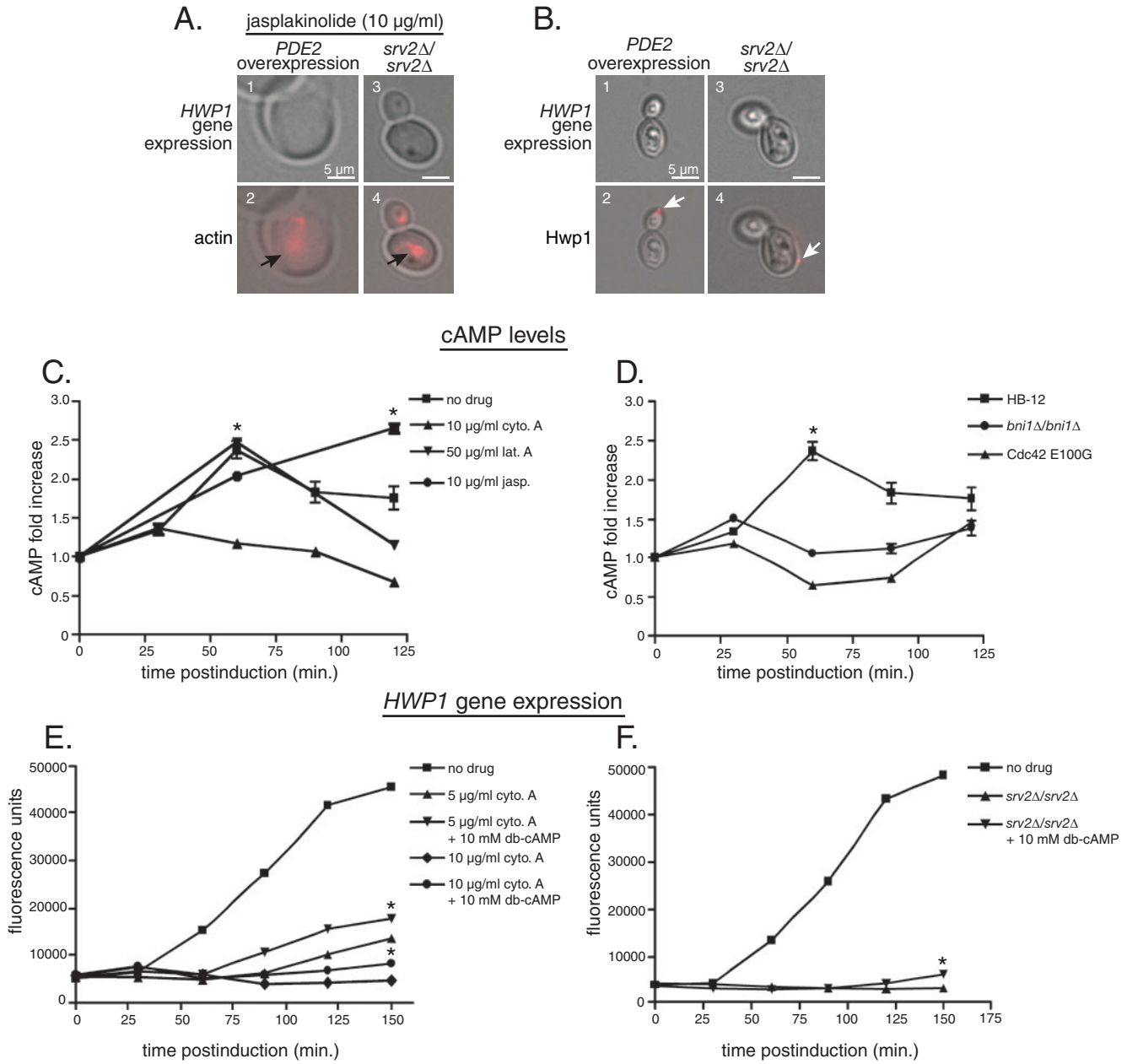

FIG. 8. Role of cAMP in actin-mediated *HWP1* gene expression. (A) *HWP1* gene expression and F-actin staining in EPDE2-3 (*PDE2* overexpression) (1 and 2) and MWY3 (*srv2*Δ/*srv2*Δ) (3 and 4) strains exposed to 10 μg/ml jasplakinolide under hypha-inducing conditions. (B) Localization of Hwp1 to a distinct region on cell surfaces of the *srv2*Δ/*srv2*Δ and *PDE2* overexpression strains (2 and 4, arrows). *HWP1* gene expression was insufficient to be detectable by measuring the fluorescence of the GFP reporter in both genetic backgrounds (1 and 3). (C) Intracellular cAMP levels of cells treated with actin-influencing agents. *, $P < 0.001$ (no drug versus 10 μg/ml cytochalasin A [cyto. A] at 60 min and no drug versus 10 μg/ml cytochalasin A, latrunculin A, and jasplakinolide at 120 min). (D) Intracellular cAMP levels of actin-compromised mutant cells. *, $P < 0.001$ (no drug versus both mutant strains at 60 min). (E) *HWP1* gene expression in the presence of 5 or 10 μg/ml cytochalasin and the presence or absence of 10 mM dibutyryl (db)-cAMP. *, $P < 0.001$ (5 μg/ml and 10 μg/ml cytochalasin A plus db-cAMP versus no dibutyryl-cAMP, at 150 min). (F) *HWP1* gene expression of strain MWY3 (*srv2*Δ/*srv2*Δ) in the presence (inverted triangles) or absence (triangles) of 10 mM dibutyryl-cAMP. *, $P < 0.01$ (with dibutyryl-cAMP versus no dibutyryl-cAMP at 150 min).

monomer sequestration may result in an overall decline of cAMP production in latrunculin A-treated cells despite the initial increase. This decline, in turn, would be reflected in a decline in *HWP1* gene expression (Fig. 1B, panels 7 to 12).

By contrast, jasplakinolide treatment (10 μg/ml) led to cAMP levels that were 75% of those in untreated cells at 60 min and surpassed levels found in untreated cells at 120 min postinduction, demonstrating a sustained gradual increase over time in cAMP levels in response to jasplakinolide-mediated stabilized actin. The sustained increase in cAMP levels seen in jasplakinolide-treated cells with stabilized actin was similar to the sustained increase previously observed

in a *pde2*Δ/*pde2*Δ strain in which cAMP degradation is inhibited (6).

Examination of intracellular cAMP levels in the *bni1*Δ/*bni1*Δ and Cdc42 E100G strains revealed a loss in the peak of cAMP production that occurred in strain HB-12 at 60 min postinduction (Fig. 8D). At the 60-min time point, the *bni1*Δ/*bni1*Δ and Cdc42 E100G strains showed cAMP levels at 46% and 26%, respectively, of the peak cAMP levels observed from HB-12. By 120 min postinduction, however, the cAMP levels in the actin-compromised mutant strains were close to HB-12 levels.

(iii) Partial recovery of *HWP1* gene expression by exogenous cAMP. The addition of 10 mM dibutyryl-cAMP to HB-12 cells treated with 5 μg/ml and 10 μg/ml cytochalasin A resulted in 1.5- and 1.75-fold increases in *HWP1*-derived GFP fluorescence following 150 min of induction, to levels that were 38% and 18% of HB-12 levels, respectively (Fig. 8E). The results were statistically significant and suggested that cAMP was able to partially rescue the effects of cytochalasin A concentrations that normally curtail hypha formation and *HWP1* gene expression. Higher concentrations of dibutyryl-cAMP did not further increase GFP reporter fluorescence. Treatment of the *srv2*Δ/*srv2*Δ strain with 10 mM dibutyryl-cAMP yielded a twofold increase in *HWP1* gene expression compared to that in untreated cells, although after partial rescue levels were only 13% of those seen in untreated HB-12 cells (Fig. 8F). These partial recoveries of *HWP1* gene expression by dibutyryl-cAMP support the relationship between actin cytoskeletal aggregates and activation of the cAMP pathway.

Together, the data show that conditions that interfere with F-actin formation also affect the kinetics of cAMP levels in wild-type cells, which peak at 60 min when polarized F-actin becomes present in cells prior to germ tube emergence, beginning at 30 min (Fig. 5A). The results suggest a correlation between the presence of stabilized actin and increasing cAMP levels during the slow phase of *HWP1* gene expression, which precedes the rapid phase of induction. The results also underscore the importance of rapid cAMP production at the bud-hypha transition prior to the fast phase of *HWP1* gene expression and the strong contribution of stabilized F-actin to the development and maintenance of this cAMP activation. F-actin aggregation alone was not sufficient to override mutations in the cAMP pathway, and the disruption of actin aggregation resulted in marked declines in intracellular cAMP levels among cytochalasin A-treated cells as well as actin-compromised mutant strains.

DISCUSSION

A major outcome from the work described in this study is the discovery that actin dynamics play a major role in activating *HWP1* gene expression. The up-regulation of *HWP1* gene expression in the presence of hyphal blockade by jasplakinolide but not cytochalasin A or latrunculin A strongly suggested that actin structures are involved in *HWP1* gene expression. The results of our studies suggested the existence of major parallels to the role of actin structures in apoptotic pathways in *S. cerevisiae*. Reductions in actin dynamics in *S. cerevisiae* caused by jasplakinolide or by mutations in genes that function in the endocytic pathway lead to the presence of large clumps of F-actin aggregates within cells that activate the cAMP signaling pathway, increase reactive oxygen species (ROS) production, and ultimately lead to apoptosis (5). Increases in oxygen radical generation during germ tube induction have also been observed in *C. albicans* (67), suggesting the possibility that changes in actin dynamics during morphogenesis may be related to the generation of oxygen radicals. Unlike the apoptotic response to stabilized actin in *S. cerevisiae*, however, the effect of jasplakinolide on *C. albicans* with respect to activating *HWP1* depended on the presence of hypha-inducing conditions. Specifically, *HWP1* gene expression did not occur in cells treated with jasplakinolide under yeast-inducing conditions despite the presence of stabilized F-actin structures (Fig. 2B). These findings strongly suggest that alterations to actin dynamics at the bud-hypha transition result in the remodeling of F-actin structures during morphogenesis that occurs simultaneously with the presence of environmental signals to activate gene expression at the *HWP1* locus.

It is important to acknowledge the potential difficulties with interpreting results from drug studies. Cytochalasin A is chemically similar to the thiol-alkylating agent N-ethylmaleimide (NEM) and has secondary effects on cell metabolism and thiol alkylation in mammalian cells that are unrelated to effects on actin (18, 32, 35). In this study, unlike studies with mammalian cells in which NEM did not interfere with actin filaments (18), NEM did in fact interfere with actin polymerization in *C. albicans* (not shown). The differential effect of NEM on actin from *C. albicans* compared to mammalian cells points to an intrinsic difference in sensitivity to oxidation between the two actins in their respective environments that may reflect the observation by us and others (32) that yeast and fungi are sensitive to cytochalasin A but not to cytochalasin B. Support for a role for oxidation in actin depolymerization is provided by recent studies showing that oxidation of mammalian actin by peroxide can cause a complete loss of polymerization potential, an effect involving cysteine 374 (40), which is conserved in *C. albicans* actin. Thus, the influence of thiol alkylation on hyphal development and *HWP1* expression does not preclude the correlation between F-actin and *HWP1* expression.

Consistent with the importance of reduced sulfhydryl groups in F-actin function, the simultaneous addition of dithiothreitol (DTT) (1 mM) and cytochalasin A (0.02 mM) prevented the complete depolymerization of actin and partially rescued *HWP1* gene expression (not shown). GFP levels attained 70% of the level seen in untreated cells in the presence of DTT and cytochalasin A, which was equivalent to GFP levels in the presence of jasplakinolide. Importantly, DTT alone also blocked germ tube formation, but actin was not depolarized or depolymerized and *HWP1* gene expression was again retained at the level of 70% of that seen in untreated cells. The effect of DTT alone on blocking germ tube formation could be explained by the selective retention of secretory proteins in the endoplasmic reticulum (25). The effect of DTT was similar to that of brefeldin A in preventing germ tube formation but not actin polymerization or *HWP1* gene expression (see below). Thus, the results of germ tube blockage using NEM, DTT, and DTT plus cytochalasin A were consistent with the correlation between the absence or presence of F-actin and the loss or presence, respectively, of *HWP1* gene expression as assessed by measuring GFP fluorescence using epifluorescence microscopy.

The importance of F-actin in *HWP1* gene expression was not solely based on treatments with cytochalasin A. Latrunculin A, an actin filament destabilizer like cytochalasin A, produced identical losses in hypha formation and *HWP1* gene expression as cytochalasin A but required higher drug concentrations (0.12 mM versus 0.02 mM) to attain them, a fact reflective of the monomer-sequestering mechanism by which latrunculin A functions (13). Jasplakinolide, an actin filament stabilizer, produced the opposite effect of the actin-destabilizing drugs. The correlation between F-actin and *HWP1* gene expression was also supported by genetic studies and kinetic analyses discussed in the previous section as well as below.

The effect of brefeldin A on hypha formation and *HWP1* gene expression is also consistent with a central role for stabilized F-actin in the regulation of both processes. Brefeldin A acts as a specific disruptor of Golgi complex-mediated secretory processes (9, 43), while leaving other cellular processes, such as those involving the actin cytoskeleton, unaltered (30). Whereas recent work has revealed that Bni1-mediated actin cables are necessary for positioning the Golgi complex to a putative site of germ tube emergence and for coordinating the transport and deposition of membrane and cell wall material to a growing hypha (65), actin dynamics would not be expected to change in response to the bud-hypha transition in cells with a chemically dispersed Golgi complex. However, we found that the loss of Golgi complex-mediated secretion prevented hypha development in cells treated with brefeldin A, implicating the Golgi complex as a central player in bud-hypha transitions. These results vary from the recently published findings of Rida et al. (65), since brefeldin A was added to cells simultaneously with the shift to hypha-inducing conditions in our experiments rather than allowing hyphal structures to develop prior to drug addition as in the study by Rida et al. (65). Addition of brefeldin A during the bud-hypha transition would not be expected to interfere with actin dynamics and subsequent expression of *HWP1*. However, the inability of these cells to form a coherent Golgi complex at the site of hypha formation (65) prevented hypha development, resulting in cells with a yeast-like morphology despite the expression of hypha-specific genes. The results using brefeldin A-treated cells further support the importance of hypha-inducing environmental conditions in *HWP1* expression as well as the idea that the yeast morphology is not incompatible with the type of actin dynamics that can promote cAMP pathway up-regulation, leading to the expression of genes that are usually hypha specific.

The effects of benomyl, propranolol, and ML-7 on hyphal development and *HWP1* gene expression may also be examined within the context of F-actin. It has been previously shown that the actin cytoskeleton is disrupted along with microtubules upon benomyl treatment (1), which accounts for the cytochalasin A- and latrunculin A-like phenotype observed in our benomyl experiment. Actin bundle disruption and filament depolymerization have also been observed in connection with the use of propranolol (23, 55) and ML-7 (36, 53), suggesting that the stabilization of F-actin may be a common explanatory thread linking the results of all seven of the drugs analyzed in this study.

The contribution of F-actin structures to *HWP1* gene expression is supported by genetic data. First, in terms of the ability to activate *HWP1*, strains lacking the formin gene *BNI1* differed markedly from strains lacking the profilin gene *PFY1* despite strong similarities in their morphological defects to hyphal cells. Specifically, *HWP1* gene expression was decreased in *bni1*Δ/*bni1*Δ cells and unaffected in *pfy1*Δ/*pfy1*Δ cells. Recent work has shown that Bni1 is localized primarily to the developing hypha tip and that its presence is necessary for the development of a wild-type hyphal structure though not for overall apical growth (41). The reduction in *HWP1* gene expression in the *bni1*Δ/*bni1*Δ mutant could be related to a compromise to the formin-mediated actin cytoskeletal network that is essential for wild-type hyphal development. While not preventing hyphal morphogenesis per se, the loss of *BNI1* may prevent the synthesis of appropriate F-actin structures necessary at the bud-hypha transition for the formation of a cell exhibiting wild-type levels of hypha-specific gene expression (41). Therefore, the finding that deletion of *BNI1* compromises *HWP1* expression both in the strain generated in this work and the strain generated by Li et al. (41) provides direct genetic evidence supporting the drug studies that specific F-actin structures contribute to *HWP1* gene expression. By contrast, loss of Pfy1 would reduce the efficiency of actin rearrangements during hyphal morphogenesis but not preclude them, allowing *HWP1* gene expression to persist in a *pfy1*Δ/*pfy1*Δ null mutant.

The importance of stabilized F-actin to the *HWP1*-regulatory process was also supported by the reduction in *HWP1* gene expression in a strain carrying a specific glutamic acid-to-glycine alteration (Cdc42 E100G) encoded by *CDC42* (78) that leads to deficient interactions with Bni1 (51). Work with *S. cerevisiae* has implicated Cdc42 as a direct mediator of actin cytoskeletal dynamics during polarized morphogenesis through its physical interactions with Bni1 (14). More-recent work suggests that this Cdc42-Bni1 interaction exists in *C. albicans* as well and that compromises to this interaction have deleterious effects on hypha formation (78). The level of *HWP1* gene expression in the Cdc42 E100G strain compared to that in HB-12 (47%) mirrored the level observed in the *bni1*Δ/*bni1*Δ strain (63%), which is consistent with the idea that formin-based actin filament rearrangements play a critical role in *HWP1* expression. Assessing further compromises to *HWP1* expression by the simultaneous deletion of both *C. albicans* formins is not possible because *C. albicans bni1*Δ/*bni1*Δ *bnr1*Δ/*bnr1*Δ cells are inviable (41).

Although the exact nature of the native actin structures that may support the expression of *HWP1* during the bud-hypha transition is not known, it is possible that F-actin aggregates that are similar to those observed in a fraction of the cells in stationary-phase cultures of *S. cerevisiae* may be present (20) except that the aggregated F-actin in germ tubes is polarized at the apex of the emerging germ tube. The possibility that overall increases in F-actin levels are involved is considered to be unlikely based on the low level of G-actin reserves in *S. cerevisiae*, which have been measured to be 1% of total actin (5). Indeed, our quantitative analysis did not reveal a difference between the level of total F-actin in cells forming nascent germ tubes or nascent buds. An alternative possibility is that F-actin from cortical patches coalesces and is incorporated into hypha-specific F-actin structures in the emerging germ tube in a manner analogous to the convergent-evolution model of filopodial initiation (76). F-actin aggregates could also arise following the dissolution of preexisting F-actin and nucleation

of new structures that would support *HWP1* gene expression. The presence of polarized F-actin that is specific to hyphal growth and is not influenced by cell cycle cues has been previously described (24). Concentrated F-actin (2) at hyphal tips may be functionally similar to jasplakinolide-induced structures, a fact that may account for the effect of jasplakinolide on *HWP1* gene expression despite the lack of germ tube development that occurs upon jasplakinolide treatment.

A possible mechanism by which F-actin contributes to *HWP1* gene expression is through involvement of the cAMP signaling pathway. The importance of activation of the cAMP signaling pathway to *HWP1* up-regulation was demonstrated in our previous work using hypo- and hypermorphic cAMP mutants (6). Here, multiple approaches pointed to a connection between F-actin and cAMP. First, the cAMP increase that normally occurs and peaks within 60 min of hypha induction was largely abrogated in the presence of cytochalasin A treatment as well as in mutants that are deficient in the nucleation of F-actin. Although latrunculin A did not inhibit the cAMP peak, cAMP levels during the fast phase of *HWP1* gene expression were significantly reduced compared to those in untreated cells after 120 min. Second, measurements of intracellular cAMP in cells treated with 10 μg/ml jasplakinolide revealed a gradual but sustained increase in cAMP levels during hypha induction that did not decline over time but rather continued to increase during the fast phase of *HWP1* gene expression. Third, the absence of Srv2 as well as the overexpression of *PDE2*, which encodes the high-affinity phosphodiesterase that degrades cAMP, led to the loss of *HWP1* gene expression in the presence of jasplakinolide-stabilized actin structures. The absence of *HWP1* gene expression despite the presence of jasplakinolide-stabilized actin in hypha-inducing conditions was consistent with the idea that elevated levels of cAMP are responsible for *HWP1* gene expression in association with F-actin. A similar experiment using overexpression of the *PDE2* gene was used in *S. cerevisiae* to demonstrate the importance of cAMP signaling in the presence of stabilized actin (20). Fourth, the addition of dibutyryl-cAMP partially reversed the genetic and chemical-genetic interference with F-actin polymerization.

The data from this study suggest that the mechanisms leading to *HWP1* gene expression share similarities to the F-actin-related increases in release of ROS from mitochondria that precede apoptosis in *S. cerevisiae*. Mutations in the *sla1* or *end3* genes (21) interfere with the actin dynamics that accompany endocytosis, stabilize F-actin, and hyperactivate the Ras/cAMP pathway. Adenylyl cyclase and the cyclase-associated protein Srv2 were observed to colocalize with stabilized actin. The colocalization of stabilized actin and cAMP pathway components was accompanied by concomitant increases in cytoplasmic cAMP levels, oxygen radicals, and apoptosis, leading to the conclusion that stabilized actin structures and hyperactivation of the cAMP signaling pathway were interrelated. Apoptosis and the presence of ROS have also been described for *C. albicans* (61, 62), and connections between these processes and germ tube formation are indicated by an increase in ROS at the time of germ tube formation (67). The incomplete rescue of *C. albicans HWP1* gene expression by dibutyryl-cAMP in the presence of genetic and chemical-genetic compromises to F-actin parallels the lower levels of ROS generated upon addition of exogenous cAMP to a *pde2* mutant compared to ROS levels generated by the endocytosis mutants of *S. cerevisiae* and is suggestive of a similar relationship between the cAMP signaling pathway and F-actin in the two organisms. The possibility that hypha-inducing conditions impact mitochondrial function is suggested by the interference of these conditions with electron transport, a shift to fermentative metabolism, and impairment in oxygen uptake (37). Finally, a recent result from the literature that is also consistent with the correlation between the presence of stabilized actin and activation of the cAMP pathway in *C. albicans* was the finding that a *C. albicans sla2*Δ/*sla2*Δ mutant did not show alterations in cAMP-regulated gene expression despite the inability to form true hyphae (58). *C. albicans sla2*Δ/*sla2*Δ null mutants would be predicted to have a block in endocytosis-associated actin dynamics and stabilization similar to that of *S. cerevisiae sla1*Δ/*sla1*Δ mutants given the related roles of Sla1p and Sla2p in *S. cerevisiae* endocytosis (52).

Despite the intriguing similarities mentioned in the previous paragraph, there are unexplained differences between pathways leading to *HWP1* gene expression and pathways leading to apoptosis in both *S. cerevisiae* and *C. albicans*. Little is known about the exact signaling mechanisms that limit *HWP1* gene expression to hypha-inducing growth conditions, the potential colocalization of the *C. albicans* cAMP pathway components Srv2 and Cyr1 (adenylyl cyclase) with aggregated F-actin, the functional roles of the *C. albicans* protein kinase A (PKA) isoforms Tpk1 and Tpk2 at the bud-hypha transition in comparison with the established roles of *S. cerevisiae* PKA isoforms in apoptosis, and the differences in F-actin organization and interactions with cAMP between *S. cerevisiae* and *C. albicans* that permit balanced hyphal growth and reversion to yeast growth conditions in the latter case. Future research to investigate these questions is likely to have a high impact on the understanding of the mechanisms of candidiasis that relate to interconversion between *C. albicans* growth morphologies.

Srv2 of *C. albicans* could be important for the coupling of F-actin dynamics and cAMP pathway activation that leads to *HWP1* gene expression (7). In this work, we found that *HWP1* was not expressed in the *srv2*Δ/*srv2*Δ mutant even though stabilized actin structures could be induced by jasplakinolide, suggesting that cAMP activation is necessary for *HWP1* gene expression and that the Srv2 protein is essential to this process. In *S. cerevisiae*, it has been shown that Srv2 localizes to actin patches at the site of endocytosis as well as to stabilized actin structures that are generated in the mutants with defects in endocytosis (21). It is possible that Srv2 serves as a sensor of changes in actin dynamics that are translated into activation of the cAMP pathway. Srv2 has been shown to consist of an N-terminal region that primarily interacts with adenylyl cyclase, a central polyproline region that indirectly interacts with F-actin via Abp1, and a C-terminal region with GDP-actin monomer binding ability that facilitates localized actin turnover (42, 48). It is logical that Srv2 could serve as a downstream signaling target for the rapid remodeling and polarization of actin filaments that takes place in response to external signals. Indeed, in the recent work previously mentioned that implicated *S. cerevisiae* actin stabilization with Ras/cAMP pathway activation (21), it was also found that Srv2 played a key role as a signaling conduit between actin filaments and the activation

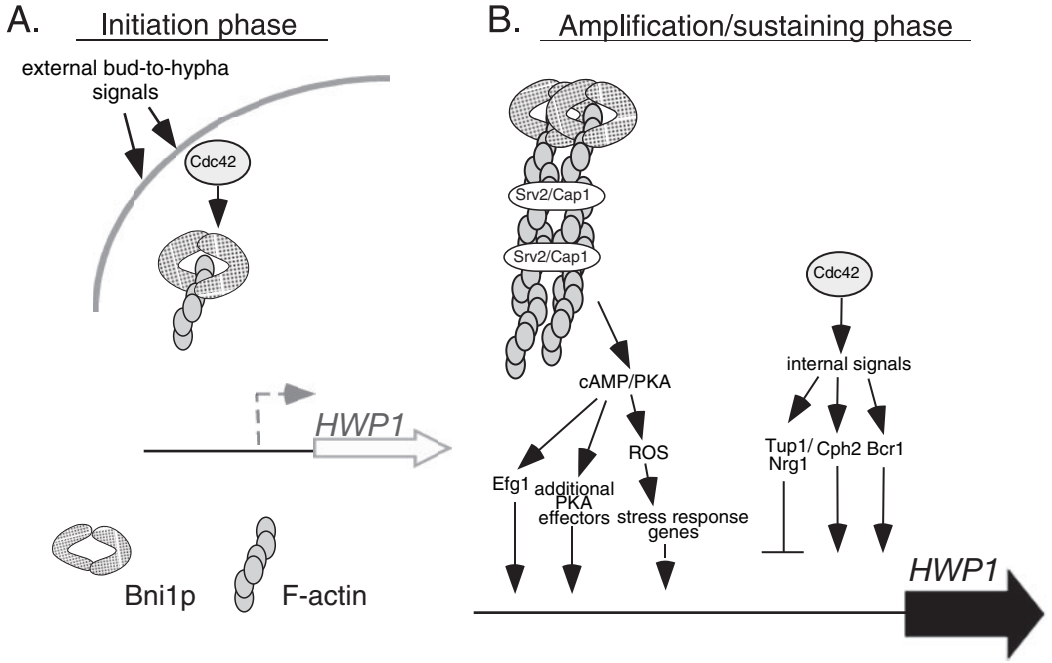

FIG. 9. Model for biphasic expression and up-regulation of *HWP1* at the bud-hypha transition. (A) In the initial-expression phase, environmental signals activate undetermined signal transduction pathways, allowing for small-scale *HWP1* gene expression as shown by the gray arrow. Stabilized actin is not required for this gene expression. This initial *HWP1* expression occurs simultaneously with polarization events resulting from Cdc42 interactions with Bni1 in conjunction with other proteins, such as Mea1p, that lead to localized Hwp1 deposition on the cell wall surface. While Cdc42 interactions with Bni1 may be promoting formin-based actin filamentation at this stage, *HWP1* gene expression is not contingent on the presence of these filaments. (B) Actin structures play a direct role in the amplification and sustaining phase. Bni1-nucleated F-actin aggregates act as a platform for Srv2/Cap1 aggregation, which in turn serves as a regulatory conduit in the activation of the cAMP pathway and its effectors, leading to the production of ROS. These cAMP/PKA effectors are joined by a number of independently up-regulated activators and down-regulated repressors (11, 27, 54, 56, 64, 69, 79) that may act upon *HWP1* in a direct or indirect manner. Work by other groups has suggested that these factors may be regulated in part by Cdc42 (46, 50, 77, 78). These changes in regulatory factor expression allow for increased *HWP1* gene expression levels in response to various environmental signals, as represented by the large black arrow.

of cAMP-related downstream effectors. This intriguing finding implies that cAMP pathway activation and up-regulation at the bud-hypha transition may promote the formation of stabilized actin structures via Srv2 interaction, thereby facilitating the presence of sustained actin polarization at the nascent germ tube and increasing *HWP1* expression. Given what has been discovered in recent years regarding the complexities of *C. albicans* regulation of hyphal morphogenesis, however, it is also likely that additional proteins that contribute to this actin-based regulatory process will be discovered.

One interesting idea raised by the production of oxygen radicals as a by-product of the bud-hypha transition is that these oxygen radicals may play a role in regulating factors that control *HWP1* gene expression. Current opinion regarding the regulation of *HWP1* is that initial activation of the Ras/cAMP pathway targets transcription factors such as Efg1 for *HWP1* activation. Based on what is known about the role of oxygen radicals and the Hog1 pathway in terms of hypha formation, it is possible that stress response genes activated in response to oxygen radical generation may contribute to *HWP1* up-regulation (49, 67). It is also possible that the Hog1 oxidative stress response pathway may control not only the level of oxygen radicals in the transitioning cell but also the overall bud-hypha structural transition since cells with a constitutively active Hog1 pathway are unable to form hyphae (49). These results, taken together, suggest that the ability of *C. albicans* to produce a spike in oxygen radicals at the bud-hypha transition (67) may represent another mechanism by which bud-hypha regulatory pathways are controlled.

Our examination of Hwp1 localization using indirect immunofluorescence revealed the presence of Hwp1 at patches on the cell surface that were predicted to represent sites of emerging hyphae. The presence of Hwp1 at localized surface patches was indicative of a low level of *HWP1* gene expression that was difficult to detect in individual cells by visualizing fluorescence from the GFP reporter and did not require the presence of stabilized actin structures. Interestingly, this initial low level of expression did not appear to require the polarization events that accompany germ tube emergence since cells induced to excise the essential *CDC42* gene were found to have surface Hwp1 localization that was not restricted to aggregated patches. Likewise, deletion of other factors that are believed to play a role in the polarization of *C. albicans* at the bud-hypha transition, such as *BNI1* or *MEA1*, affected Hwp1 localization but did not prevent low-level *HWP1* gene expression. A role for the cAMP signaling pathway in the initial stage of *HWP1* gene expression was not found. The *srv2*Δ/*srv2*Δ mutant exhibited localized surface Hwp1 that was indistinguishable from that of HB-12. The central role played by Cdc42 in the initial stages of the bud-hypha transition argues that additional *CDC42*-mediated pathways beyond *BNI1* play key roles in the activation of *HWP1* gene expression. These additional path-

ways may include as yet unidentified linkages between Cdc42 and critical bud-hypha transition downstream effectors, including modifiers of actin architecture such as the Arp2/3 complex activator Wal1, the transcriptional activators Cph2 and Tec1, and the transcriptional repressors Tup1 and Nrg1 (44, 46). Additional study of Cdc42-mediated regulation of the bud-hypha transition is necessary to develop a complete picture of the complex interactions that take place between these pathways in the regulation of hypha-specific transcripts like *HWP1*.

It is important to note that this study has focused exclusively on the *HWP1* gene as a model for hypha-specific gene regulation in *C. albicans*. Nevertheless, these findings may reflect a more general model of biphasic hypha-specific gene expression. Indeed, the hypha-specific adhesin Als3 is known to share a similar promoter structure and set of candidate regulatory factors with Hwp1 (3), suggesting the possibility for actin-influenced regulation at this locus as well.

Another major finding from this work is the recognition of a new role for F-actin in *C. albicans*, which is already known to be essential for hyphal growth (1) and is enriched in the region of the Spitzenkörper (12), a structure whose position in the growing hypha determines the directionality of growth. Our studies suggest that F-actin structures form a close interrelationship with the cAMP signaling pathway and serve to upregulate the synthesis of cAMP, thereby activating the expression of *HWP1* and potentially other hypha-specific genes. Thus, our chemical-genetic and genetic approaches provide a mechanistic explanation for the close correlation between cytoskeletal dynamics during morphogenesis and hypha-specific gene expression. This finding is consistent with work in mammalian cells that also suggests that actin rearrangements can directly influence genetic regulation programs (34).

The indirect immunofluorescence and kinetic experiments described in this study delineate the steps in a pathway of developmental regulation of hypha formation in *C. albicans* (Fig. 9). The initial stage corresponds to the slow phase from the kinetics studies and is characterized by polarization events at the site of emergence of the nascent hypha that are accompanied by deposition of Hwp1 and possibly other developmentally regulated proteins. The treatment of cells with drugs that destabilized or did not permit formation of F-actin blocks the onset of the second phase. Little is known about the mechanisms mediating the initial stage of germ tube polarization events; however, the formation of F-actin and the activation of the cAMP pathway are not required. The second stage in the pathway corresponds to the fast phase from the kinetics studies. This phase is dependent on F-actin aggregation that normally coincides with germ tube elongation but can be artificially replaced by drug treatment that stabilizes F-actin prior to the turnover that is required for restructuring the cytoskeleton to facilitate hyphal growth. F-actin during germ tube formation is interrelated with the activation of the cAMP signaling pathway and a high level of amplification of *HWP1* gene expression. More research is required to elucidate the factors involved in initiation of this developmental pathway and to define the molecular mechanisms that link cAMP activation to the actin cytoskeleton. The findings also pose multiple questions regarding the downstream effects of cAMP signaling that ultimately lead to *HWP1* gene expression. Interruption of these processes will ultimately lead to new strategies for disrupting the regulatory circuits that connect morphogenesis to the expression of virulence genes in *C. albicans*.

ACKNOWLEDGMENTS

Support for this research was generously provided from the National Institute of Allergy and Infectious Diseases (R01 AI46608). P. Sundstrom is a recipient of a Scholar Award from the Burroughs Wellcome Fund.

We are grateful to Julia Köhler (Children's Hospital, Boston, MA) for providing the nourseothricin flipper cassette constructs and to Joachim Morschhäuser (Universität Würzburg, Würzburg, Germany) for strains SMC7A and SMC8A and for his advice on the transformation process. We also thank Douglas Johnson (University of Vermont, Burlington) for the strains containing alterations in Cdc42. We thank Laura J. Gordon for excellent technical assistance.

REFERENCES

1. **Akashi, T., T. Kanbe, and K. Tanaka.** 1994. The role of the cytoskeleton in the polarized growth of the germ tube in *Candida albicans*. Microbiology **140:**271–280.
2. **Anderson, J. M., and D. R. Soll.** 1986. Differences in actin localization during bud and hypha formation in the yeast *Candida albicans*. J. Gen. Microbiol. **132:**2035–2047.
3. **Argimon, S., J. A. Wishart, R. Leng, S. Macaskill, A. Mavor, T. Alexandris, S. Nicholls, A. W. Knight, B. Enjalbert, R. Walmsley, F. C. Odds, N. A. Gow, and A. J. Brown.** 2007. Developmental regulation of an adhesin gene during cellular morphogenesis in the fungal pathogen *Candida albicans*. Eukaryot. Cell **6:**682–692.
4. **Arnaud, M. B., M. C. Costanzo, M. S. Skrzypek, G. Binkley, C. Lane, S. R. Miyasato, and G. Sherlock.** 2005. The *Candida* Genome Database (CGD), a community resource for *Candida albicans* gene and protein information. Nucleic Acids Res. **33:**D358–D363.
5. **Ayscough, K. R.** 2000. Endocytosis and the development of cell polarity in yeast require a dynamic F-actin cytoskeleton. Curr. Biol. **10:**1587–1590.
6. **Bahn, Y. S., J. Staab, and P. Sundstrom.** 2003. Increased high-affinity phosphodiesterase *PDE2* gene expression in germ tubes counteracts *CAP1*-dependent synthesis of cyclic AMP, limits hypha production and promotes virulence of *Candida albicans*. Mol. Microbiol. **50:**391–409.
7. **Bahn, Y. S., and P. Sundstrom.** 2001. *CAP1*, an adenylate cyclase-associated protein gene, regulates bud-hypha transitions, filamentous growth, and cyclic AMP levels and is required for virulence of *Candida albicans*. J. Bacteriol. **183:**3211–3223.
8. **Baker, C. A., K. Desrosiers, and J. W. Dolan.** 2002. Propranolol inhibits hyphal development in *Candida albicans*. Antimicrob. Agents Chemother. **46:**3617–3620.
9. **Bershadsky, A. D., and A. H. Futerman.** 1994. Disruption of the Golgi apparatus by brefeldin A blocks cell polarization and inhibits directed cell migration. Proc. Natl. Acad. Sci. USA **91:**5686–5689.
10. **Bubb, M. R., A. M. Senderowicz, E. A. Sausville, K. L. Duncan, and E. D. Korn.** 1994. Jasplakinolide, a cytotoxic natural product, induces actin polymerization and competitively inhibits the binding of phalloidin to F-actin. J. Biol. Chem. **269:**14869–14871.
11. **Cao, F., S. Lane, P. P. Raniga, Y. Lu, Z. Zhou, K. Ramon, J. Chen, and H. Liu.** 2006. The Flo8 transcription factor is essential for hyphal development and virulence in *Candida albicans*. Mol. Biol. Cell **17:**295–307.
12. **Crampin, H., K. Finley, M. Gerami-Nejad, H. Court, C. Gale, J. Berman, and P. Sudbery.** 2005. *Candida albicans* hyphae have a Spitzenkörper that is distinct from the polarisome found in yeast and pseudohyphae. J. Cell Sci. **118:**2935–2947.
13. **de Oliveira, C. A., and B. Mantovani.** 1988. Latrunculin A is a potent inhibitor of phagocytosis by macrophages. Life Sci. **43:**1825–1830.
14. **Evangelista, M., K. Blundell, M. S. Longtine, C. J. Chow, N. Adames, J. R. Pringle, M. Peter, and C. Boone.** 1997. Bni1p, a yeast formin linking Cdc42p and the actin cytoskeleton during polarized morphogenesis. Science **276:**118–122.
15. **Evangelista, M., D. Pruyne, D. C. Amberg, C. Boone, and A. Bretscher.** 2002. Formins direct Arp2/3-independent actin filament assembly to polarize cell growth in yeast. Nat. Cell Biol. **4:**260–269.
16. **Fedor-Chaiken, M., R. J. Deschenes, and J. R. Broach.** 1990. *SRV2*, a gene required for RAS activation of adenylate cyclase in yeast. Cell **61:**329–340.
17. **Fonzi, W. A., and M. Y. Irwin.** 1993. Isogenic strain construction and gene mapping in *Candida albicans*. Genetics **134:**717–728.
18. **Freed, B. M., N. Lempert, and D. A. Lawrence.** 1989. The inhibitory effects of N-ethylmaleimide, colchicine and cytochalasins on human T-cell functions. Int. J. Immonupharmacol. **11:**459–465.
19. **Gillum, A. M., E. Y. Tsay, and D. R. Kirsch.** 1984. Isolation of the *Candida albicans* gene for orotidine-5′-phosphate decarboxylase by complementation of *S. cerevisiae ura3* and E. coli *pyrF* mutations. Mol. Gen. Genet. **198:**179–182.

20. **Gourlay, C. W., and K. R. Ayscough.** 2005. Identification of an upstream regulatory pathway controlling actin-mediated apoptosis in yeast. J. Cell Sci. **118:**2119–2132.
21. **Gourlay, C. W., and K. R. Ayscough.** 2006. Actin-induced hyperactivation of the Ras signaling pathway leads to apoptosis in *Saccharomyces cerevisiae*. Mol. Cell. Biol. **26:**6487–6501.
22. **Gupta, K., J. Bishop, A. Peck, J. Brown, L. Wilson, and D. Panda.** 2004. Antimitotic antifungal compound benomyl inhibits brain microtubule polymerization and dynamics and cancer cell proliferation at mitosis, by binding to a novel site in tubulin. Biochemistry **43:**6645–6655.
23. **Ha, K. S., and J. H. Exton.** 1993. Activation of actin polymerization by phosphatidic acid derived from phosphatidylcholine in IIC9 fibroblasts. J. Cell Biol. **123:**1789–1796.
24. **Hazan, I., M. Sepulveda-Becerra, and H. Liu.** 2002. Hyphal elongation is regulated independently of cell cycle in *Candida albicans*. Mol. Biol. Cell **13:**134–145.
25. **Jamsa, E., M. Simonen, and M. Makarow.** 1994. Selective retention of secretory proteins in the yeast endoplasmic reticulum by treatment of cells with a reducing agent. Yeast **10:**355–370.
26. **Johnson, D. I.** 1999. Cdc42: An essential Rho-type GTPase controlling eukaryotic cell polarity. Microbiol. Mol. Biol. Rev. **63:**54–105.
27. **Kadosh, D., and A. D. Johnson.** 2005. Induction of the *Candida albicans* filamentous growth program by relief of transcriptional repression: a genome-wide analysis. Mol. Biol. Cell **16:**2903–2912.
28. **Karpova, T. S., J. G. McNally, S. L. Moltz, and J. A. Cooper.** 1998. Assembly and function of the actin cytoskeleton of yeast: relationships between cables and patches. J. Cell Biol. **142:**1501–1517.
29. **Kim, S., M. J. Wolyniak, J. F. Staab, and P. Sundstrom.** 2007. A 368-base-pair *cis*-acting *HWP1* promoter region, HCR, of *Candida albicans* confers hypha-specific gene regulation and binds architectural transcription factors Nhp6 and Gcf1p. Eukaryot. Cell **6:**693–709.
30. **Klausner, R. D., J. G. Donaldson, and J. Lippincott-Schwartz.** 1992. Brefeldin A: insights into the control of membrane traffic and organelle structure. J. Cell Biol. **116:**1071–1080.
31. **Kumamoto, C. A., and M. D. Vinces.** 2005. Contributions of hyphae and hypha-co-regulated genes to *Candida albicans* virulence Cell. Microbiol. **7:**1546–1554.
32. **Kuo, S. C., and J. O. Lampen.** 1975. Action of cytochalasin A, a sulfhydryl-reactive agent, on sugar metabolism and membrane-bound adenosine triphosphatase of yeast. Biochim. Biophys. Acta **389:**143–153.
33. **Kurzai, O., C. Schmitt, E. Brocker, M. Frosch, and A. Kolb-Maurer.** 2005. Polymorphism of *Candida albicans* is a major factor in the interaction with human dendritic cells. Int. J. Med. Microbiol. **295:**121–127.
34. **Kusner, D. J., J. A. Barton, K. K. Wen, X. Wang, P. A. Rubenstein, and S. S. Iyer.** 2002. Regulation of phospholipase D activity by actin. Actin exerts bidirectional modulation of mammalian phospholipase D activity in a polymerization-dependent, isoform-specific manner. J. Biol. Chem. **277:**50683–50692.
35. **Lagunoff, D.** 1976. The reaction of cytochalasin A with sulfhydryl groups. Biochem. Biophys. Res. Commun. **73:**727–732.
36. **Lamb, N. J., A. Fernandez, M. A. Conti, R. Adelstein, D. B. Glass, W. J. Welch, and J. R. Feramisco.** 1988. Regulation of actin microfilament integrity in living nonmuscle cells by the cAMP-dependent protein kinase and the myosin light chain kinase. J. Cell Biol. **106:**1955–1971.
37. **Land, G. A., W. C. McDonald, R. L. Stjernholm, and T. L. Friedman.** 1975. Factors affecting filamentation in *Candida albicans*: relationship of the uptake and distribution of proline to morphogenesis. Infect. Immun. **11:**1014–1023.
38. **Lane, S., C. Birse, S. Zhou, R. Matson, and H. Liu.** 2001. DNA array studies demonstrate convergent regulation of virulence factors by Cph1, Cph2, and Efg1 in *Candida albicans*. J. Biol. Chem. **276:**48988–48996.
39. **Lane, S., S. Zhou, T. Pan, Q. Dai, and H. Liu.** 2001. The basic helix-loop-helix transcription factor Cph2 regulates hyphal development in *Candida albicans* partly via TEC1. Mol. Cell. Biol. **21:**6418–6428.
40. **Lassing, I., F. Schmitzberger, M. Bjornstedt, A. Holmgren, P. Nordlund, C. E. Schutt, and U. Lindberg.** 2007. Molecular and structural basis for redox regulation of beta-actin. J. Mol. Biol. **370:**331–348.
41. **Li, C. R., Y. M. Wang, X. De Zheng, H. Y. Liang, J. C. Tang, and Y. Wang.** 2005. The formin family protein CaBni1p has a role in cell polarity control during both yeast and hyphal growth in *Candida albicans*. J. Cell Sci. **118:**2637–2648.
42. **Lila, T., and D. G. Drubin.** 1997. Evidence for physical and functional interactions among two *Saccharomyces cerevisiae* SH3 domain proteins, an adenylyl cyclase-associated protein and the actin cytoskeleton. Mol. Biol. Cell **8:**367–385.
43. **Lippincott-Schwartz, J., L. C. Yuan, J. S. Bonifacino, and R. D. Klausner.** 1989. Rapid redistribution of Golgi proteins into the ER in cells treated with brefeldin A: evidence for membrane cycling from Golgi to ER. Cell **56:**801–813.
44. **Liu, H.** 2001. Transcriptional control of dimorphism in *Candida albicans*. Curr. Opin. Microbiol. **4:**728–735.
45. **Makishima, M., Y. Honma, M. Hozumi, K. Sampi, M. Hattori, and K. Motoyoshi.** 1991. Induction of differentiation of human leukemia cells by inhibitors of myosin light chain kinase. FEBS Lett. **287:**175–177.
46. **Martin, R., A. Walther, and J. Wendland.** 2005. Ras1-induced hyphal development in *Candida albicans* requires the formin Bni1. Eukaryot. Cell **4:**1712–1724.
47. **Mateus, C., and S. V. Avery.** 2000. Destabilized green fluorescent protein for monitoring dynamic changes in yeast gene expression with flow cytometry. Yeast **16:**1313–1323.
48. **Mattila, P. K., O. Quintero-Monzon, J. Kugler, J. B. Moseley, S. C. Almo, P. Lappalainen, and B. L. Goode.** 2004. A high-affinity interaction with ADP-actin monomers underlies the mechanism and in vivo function of Srv2/cyclase-associated protein. Mol. Biol. Cell **15:**5158–5171.
49. **Menon, V., D. Li, N. Chauhan, R. Rajnarayanan, A. Dubrovska, A. H. West, and R. Calderone.** 2006. Functional studies of the Ssk1p response regulator protein of *Candida albicans* as determined by phenotypic analysis of receiver domain point mutants. Mol. Microbiol. **62:**997–1013.
50. **Michel, S., S. Ushinsky, B. Klebl, E. Leberer, D. Thomas, M. Whiteway, and J. Morschhäuser.** 2002. Generation of conditional lethal *Candida albicans* mutants by inducible deletion of essential genes. Mol. Microbiol. **46:**269–280.
51. **Mösch, H. U., T. Kohler, and G. H. Braus.** 2001. Different domains of the essential GTPase Cdc42p required for growth and development of *Saccharomyces cerevisiae*. Mol. Cell. Biol. **21:**235–248.
52. **Moseley, J. B., and B. L. Goode.** 2006. The yeast actin cytoskeleton: from cellular function to biochemical mechanism. Microbiol. Mol. Biol. Rev. **70:**605–645.
53. **Murthy, K., and P. Wadsworth.** 2005. Myosin-II-dependent localization and dynamics of F-actin during cytokinesis. Curr. Biol. **15:**724–731.
54. **Nantel, A., D. Dignard, C. Bachewich, D. Harcus, A. Marcil, A. P. Bouin, C. W. Sensen, H. Hogues, M. van het Hoog, P. Gordon, T. Rigby, F. Benoit, D. C. Tessier, D. Y. Thomas, and M. Whiteway.** 2002. Transcription profiling of *Candida albicans* cells undergoing the yeast-to-hyphal transition. Mol. Biol. Cell **13:**3452–3465.
55. **Nicotra, A., and G. Schatten.** 1990. Propranolol, a beta-adrenergic receptor blocker, affects microfilament organization, but not microtubules, during the first division in sea urchin eggs. Cell Motil. Cytoskel. **16:**182–189.
56. **Nobile, C. J., and A. P. Mitchell.** 2005. Regulation of cell-surface genes and biofilm formation by the *C. albicans* transcription factor Bcr1p. Curr. Biol. **15:**1150–1155.
57. **Oberholzer, U., A. Marcil, E. Leberer, D. Y. Thomas, and M. Whiteway.** 2002. Myosin I is required for hypha formation in *Candida albicans*. Eukaryot. Cell **1:**213–238.
58. **Oberholzer, U., A. Nantel, J. Berman, and M. Whiteway.** 2006. Transcript profiles of *Candida albicans* cortical actin patch mutants reflect their cellular defects: contribution of the Hog1p and Mkc1p signaling pathways. Eukaryot. Cell **5:**1252–1265.
59. **Ostrander, D. B., and J. A. Gorman.** 1997. Isolation and characterization of the *Candida albicans PFY1* gene for profilin. Yeast **13:**871–880.
60. **Pearson, C. L., K. Xu, K. E. Sharpless, and S. D. Harris.** 2004. MesA, a novel fungal protein required for the stabilization of polarity axes in *Aspergillus nidulans*. Mol. Biol. Cell **15:**3658–3672.
61. **Phillips, A. J., J. D. Crowe, and M. Ramsdale.** 2006. Ras pathway signaling accelerates programmed cell death in the pathogenic fungus *Candida albicans*. Proc. Natl. Acad. Sci. USA **103:**726–731.
62. **Phillips, A. J., I. Sudbery, and M. Ramsdale.** 2003. Apoptosis induced by environmental stresses and amphotericin B in *Candida albicans*. Proc. Natl. Acad. Sci. USA **100:**14327–14332.
63. **Reuß, O., A. Vik, R. Kolter, and J. Morschhäuser.** 2004. The SAT1 flipper, an optimized tool for gene disruption in *Candida albicans*. Gene **341:**119–127.
64. **Richard, M. L., C. J. Nobile, V. M. Bruno, and A. P. Mitchell.** 2005. *Candida albicans* biofilm-defective mutants. Eukaryot. Cell **4:**1493–1502.
65. **Rida, P. C., A. Nishikawa, G. Y. Won, and N. Dean.** 2006. Yeast-to-hyphal transition triggers formin-dependent Golgi localization to the growing tip in *Candida albicans*. Mol. Biol. Cell **17:**4364–4378.
66. **Sanz, M., L. Carrano, C. Jimenez, G. Candiani, J. A. Trilla, A. Duran, and C. Roncero.** 2005. *Candida albicans* strains deficient in CHS7, a key regulator of chitin synthase III, exhibit morphogenetic alterations and attenuated virulence. Microbiology **151:**2623–2636.
67. **Schröter, C., U. C. Hipler, A. Wilmer, W. Kunkel, and U. Wollina.** 2000. Generation of reactive oxygen species by *Candida albicans* in relation to morphogenesis. Arch. Dermatol. Res. **292:**260–264.
68. **Scott, V. R., R. Boehme, and T. R. Matthews.** 1988. New class of antifungal agents: jasplakinolide, a cyclodepsipeptide from the marine sponge, *Jaspis* species. Antimicrob. Agents Chemother. **32:**1154–1157.
69. **Sharkey, L. L., M. D. McNemar, S. M. Saporito-Irwin, P. S. Sypherd, and W. A. Fonzi.** 1999. *HWP1* functions in the morphological development of *Candida albicans* downstream of *EFG1*, *TUP1*, and *RBF1*. J. Bacteriol. **181:**5273–5279.
70. **Shen, J., W. Guo, and J. R. Köhler.** 2005. CaNAT1, a heterologous dominant selectable marker for transformation of *Candida albicans* and other pathogenic *Candida* species. Infect. Immun. **73:**1239–1242.

71. **Snide, J. L., and P. Sundstrom.** 2006. A characterization of HWP1 promoter activation in pseudohyphal cells in *Candida albicans*, abstr. C192, p. 103. Abstr. 8th Candida Candidiasis, Denver, CO. American Society for Microbiology, Washington, DC.
72. **Staab, J. F., Y. S. Bahn, and P. Sundstrom.** 2003. Integrative, multifunctional plasmids for hypha-specific or constitutive expression of green fluorescent protein in *Candida albicans*. Microbiology **149:**2977–2986.
73. **Staab, J. F., Y. S. Bahn, C. H. Tai, P. F. Cook, and P. Sundstrom.** 2004. Expression of transglutaminase substrate activity on *Candida albicans* germ tubes through a coiled, disulfide-bonded N-terminal domain of Hwp1 requires C-terminal glycosylphosphatidylinositol modification. J. Biol. Chem. **279:**40737–40747.
74. **Staab, J. F., C. A. Ferrer, and P. Sundstrom.** 1996. Developmental expression of a tandemly repeated, proline- and glutamine-rich amino acid motif on hyphal surfaces on *Candida albicans*. J. Biol. Chem. **271:**6298–6305.
75. **Sundstrom, P. M., and G. E. Kenny.** 1984. Characterization of antigens specific to the surface of germ tubes of *Candida albicans* by immunofluorescence. Infect. Immun. **43:**850–855.
76. **Svitkina, T. M., E. A. Bulanova, O. Y. Chaga, D. M. Vignjevic, S. Kojima, J. M. Vasiliev, and G. G. Borisy.** 2003. Mechanism of filopodia initiation by reorganization of a dendritic network. J. Cell Biol. **160:**409–421.
77. **Ushinsky, S. C., D. Harcus, J. Ash, D. Dignard, A. Marcil, J. Morchhäuser, D. Y. Thomas, M. Whiteway, and E. Leberer.** 2002. *CDC42* is required for polarized growth in the human pathogen *Candida albicans*. Eukaryot. Cell **1:**95–104.
78. **vandenBerg, A. L., A. S. Ibrahim, J. E. Edwards, Jr., K. A. Toenjes, and D. I. Johnson.** 2004. Cdc42p GTPase regulates the budded-to-hyphal-form transition and expression of hypha-specific transcripts in *Candida albicans*. Eukaryot. Cell **3:**724–734.
79. **Whiteway, M.** 2000. Transcriptional control of cell type and morphogenesis in *Candida albicans*. Curr. Opin. Microbiol. **3:**582–588.